

UNEVEN TURNS OSCILLATING HEAT PIPES

A Thesis presented to the Faculty of the Graduate School

University of Missouri – Columbia

In Partial Fulfillment

Of the Requirements for the Degree

Master of Science

By

Aaron A. Hathaway

Dr. Hongbin Ma, Thesis Supervisor

MAY, 2008

The undersigned appointed by the dean of the Graduate School have examined the thesis entitled

UNEVEN TURN OSCILLATING HEAT PIPES

presented by Aaron A. Hathaway,

a candidate for the degree of Master of Science,

and hereby certify that, in their opinion, it is worthy of acceptance.

Professor Hongbin Ma

Professor Gary Solbrekken

Professor Adam Helfer

Dedication

To my parents

For teaching me to stand on my own two feet and to always follow my dreams.

Acknowledgements

I would like to acknowledge those who aided me in my work. Dr. Ma for his help in design and knowledge of heat pipes. Corey Wilson and Brian Borgmeyer for their help in the construction and testing of the heat pipes presented in this thesis. Lastly I would like to thank Brian Samuels and Rex Gish for their help during the design and manufacturing stages of my projects.

UNEVEN TURN OSCILLATING HEAT PIPES

Aaron A. Hathaway

Dr. Hongbin Ma, Thesis Supervisor

Abstract

An experimental investigation on oscillating heat pipes with uneven turns was conducted in order to determine the effect of short turns on the heat transport capability. The shorter turns do not go through both the evaporating and condensing sections; the short turns were placed only in the evaporating section. The design of the OHP consists of 14 long turns which run from the evaporator to the condenser and 6 short turns were placed only on the evaporating section. An extensive experimental investigation on the effects of the input power, tilted angle, condensing temperature, and charging ratio was conducted. Experimental results show that for all test conditions, the OHP functions very well and it can transport an input power up to 1200 W and can reach a thermal resistance of $0.028^{\circ}\text{C}/\text{W}$. From the experimental results of tilted angle effect, it can be found that the heat pipe is almost independent of the tilted angle. Most importantly, it is shown that with a number of short turns placed on the evaporating section, the OHP can operate efficiently without the assistance of the gravitational force. In other words, the heat pipe developed herein can operate at a condition of the heating section on the top and the cooling section on the bottom with a distance of 18.5 cm from the center of the evaporator section to the center of the condensing section. In addition, the results show that the heat transfer performance depends on the operating temperature and charging ratio. When the operating temperature increases, the heat transfer performance of the OHP investigated herein significantly increase.

Table of Contents

Dedication	
Acknowledgements	ii
Abstract	iii
List of Figures	vi
List of Tables	viii
Nomenclature	ix
Chapter 1	1
Introduction.....	1
Chapter 2	4
Prototype Development.....	4
Chapter 3	11
Experimental Setup and Procedure.....	11
Setup Overview.....	11
Condenser.....	11
Evaporator.....	12
Chapter 4	14
Results and Discussion.....	14
Prototype I.....	14
Prototype II.....	16
Prototype II Results.....	18
Chapter 5	43
Conclusions	43

References..... 45

List of Figures

Fig 1.1 Schematic of an Oscillating Heat Pipe.....	2
Fig 2.1 Oscillating Heat Pipe.....	6
Fig 2.2 Cooling and heating blocks for Uneven Turns OHP during assembly	8
Fig. 2.3 Uneven Turns OHP schematic design.....	9
Fig. 2.4 Prototype II after assembly.....	10
Fig 3.1 Experimental Setup.....	13
Fig. 4.1 Power input effect and the thermal resistance of the OHP	15
Fig 4.2 Aluminum condenser block.....	17
Fig. 4.3 Power input effect on the heat transfer performance in an OHP.....	19
Fig. 4.4 Power input effect on the heat transfer performance in an OHP.....	20
Fig. 4.5 Power input effect on the heat transfer performance in an OHP.....	21
Fig. 4.6 Power input effect on the heat transfer performance in an OHP.....	22
Fig. 4.7 Power input effect on the heat transfer performance in an OHP.....	23
Fig. 4.8 Power input effect on the heat transfer performance in an OHP.....	24
Fig. 4.9 Power input effect and the thermal resistance of the OHP.....	27
Fig. 4.10 Power input effect and the thermal resistance of the OHP.....	28
Fig. 4.11 Power input effect and the thermal resistance of the OHP.....	29
Fig. 4.12 Power input effect and the thermal resistance of the OHP.....	30
Fig. 4.13 Power input effect and the thermal resistance of the OHP.....	31
Fig. 4.14 Power input effect and the thermal resistance of the OH.....	32
Fig. 4.15 Power input effect and the thermal resistance of the OHP.....	33

Fig. 4.16 Power input effect and the thermal resistance of the OHP.....	34
Fig. 4.17 Power input effect and the thermal resistance of the OHP.....	35
Fig. 4.18 Power input effect and the thermal resistance of the OHP.....	36
Fig. 4.19 Power input effect and the thermal resistance of the OHP.....	37
Fig. 4.20 Power input effect and the thermal resistance of the OHP.....	38
Fig. 4.21 Temperature oscillation with respect to time.....	39
Fig. 4.22 Temperature oscillation with respect to time.....	40
Fig. 4.23 Temperature oscillation with respect to time.....	41
Fig. 4.24 Temperature oscillation with respect to time.....	42

List of Tables

Fig. 4.1 Test Configurations.....	17
-----------------------------------	----

Nomenclature

Bo Bond number

D Diameter (m)

g Gravitational acceleration (m/s^2)

P Electrical Power (W)

Q Heat transfer rate (W)

R Thermal Resistance (K/W), Electrical Resistance (Ω)

T Temperature ($^{\circ}C$)

V Voltage (V)

Greek

σ Surface tension (N/m)

ρ Density (kg/m^3)

Subscript

c Condenser

e Evaporator

l Liquid

v Vapor

Chapter 1

Introduction

With each succeeding generation of electronic systems either the package shrinks in size or the energy usage of the system increases. This leads to an increase in the power density of the system; as a result traditional low cost methods of electronics cooling are becoming unable to effectively manage the thermal issues and meet the demand of new systems. Therefore new methods of cooling these systems are being sought. One of the low cost cooling technologies currently at the fore front of the effort is the heat pipe. The heat pipe was originally developed in the 1960s and due to its flexibility in design is used in systems ranging from nuclear reactors to desktop computers. However the conventional heat pipe is having difficulty meeting the needs of these new systems. In 1990 a new type of heat pipe which is called the oscillating heat pipe (OHP), was invented and patented by Akachi [1]. The OHP unlike conventional heat pipes which transfers heat from the evaporator to the condenser as latent heat, instead transfers the heat as sensible and latent heat. The OHP operates by the expansion and contraction vapor bubbles pushing liquid plugs and vapor bubbles from the evaporator to the condenser and then pulling the plugs back to the evaporator.

OHPs are formed from a series of inter-connected channels that cross back and forth between the evaporator and condenser regions as shown in Fig. 1.1. The OHP is charged with fluid to a specific ratio of liquid volume to total fluid volume. The hydraulic diameter of the channel must be small enough that the fluid can form a complete meniscus across the channel in order for the fluid to form vapor bubbles and liquid plugs. If the hydraulic diameter of the channel is too large that the fluid will not form a

meniscus in the channel and the vapor will expand and flow over the fluid from the evaporator to the condenser. The liquid plugs and vapor bubbles should arrange themselves in a way similar to that shown in Fig. 1.1.

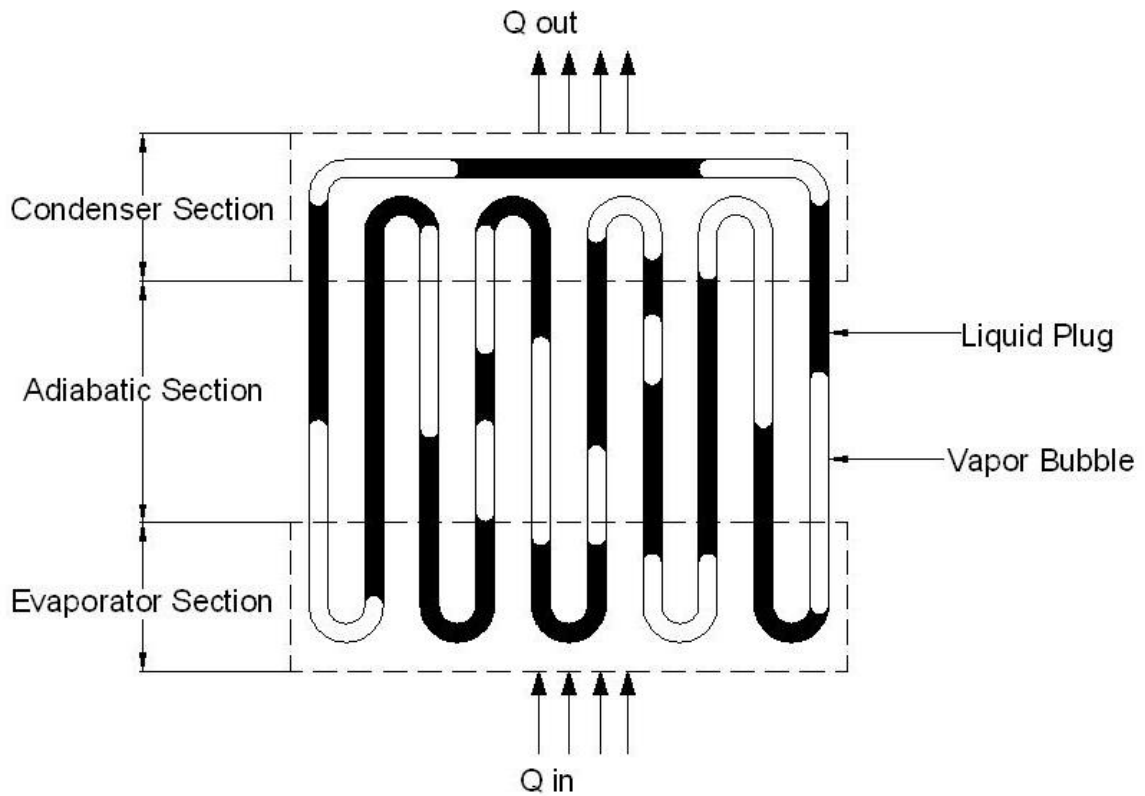


Figure 1.1 Schematic of oscillating heat pipe(The black areas are the liquid plugs and the white areas are the vapor bubbles)

The oscillating motion that occurs in a heat pipe is due to the random distribution of vapor bubbles and liquid plugs through the heat pipe, the pressure imbalance produced by the uneven expansion of the vapor bubbles in the evaporator and their contraction in the condenser region will cause the oscillating motion to occur. Extensive investigations on the oscillating heat pipe have been conducted experimentally and theoretically. These investigations [4-7] demonstrate that a system will not be able to startup and operate efficiently without the assistance of gravity to pump the fluid from the condenser to the

evaporator. In the current investigation, an innovative oscillating heat pipe, which can operate efficiently without the assistance of gravity to pump the working fluid, is investigated.

Chapter 2

Prototype Development

The hydraulic diameter of the channels utilized to form an oscillating heat pipe must be small enough that the fluid that is used to charge the oscillating heat pipe is able to form a complete meniscus across the channel preventing the flow of vapor along the channel. The maximum hydraulic diameter of the channel can be calculated utilizing

$$D_{\max} = \sqrt{\frac{Bo_{crit} \sigma}{g(\rho_l - \rho_v)}} \quad (2.1)$$

where Bo_{crit} is the critical bond number, σ is the surface tension of the fluid, ρ_l is the fluid density, ρ_v is the vapor density, and g is the gravitational acceleration. Shafii et al. [3] uses a critical Bond number of 1.84 while Khandekar et al. [2] uses a Bond number of 2. For the designs presented a Bond number of 1.84 will be used.

Two oscillating heat pipes were designed and tested. The initial concept design was tested using copper plates retasked from a previously manufactured OHP designed by Wilson et al. [10]. The total length of the system is 165.1 mm with an adiabatic section of 50.8 mm long. The evaporator was designed to be 38.1 mm long by 152.4 mm wide by 6.35 mm thick. The condenser was designed to be 63.5 mm long by 152.4 mm wide by 6.35 mm thick. The evaporator and condenser blocks were manufactured from alloy 145 copper. The initial motivation for this design was to determine if increasing the amount of time that liquid plugs spent in the evaporator would lead to greater efficiency in the transport of energy from the evaporator to the condenser. The tubing used to form

the OHP was, Alloy 122 copper tubing, with an outer diameter of 3.18 mm, and an inner diameter of 1.65 mm. This tubing meets the criteria imposed by Eq. (2.1). The tubing was attached to Alloy 145 copper plates which were used to form the evaporator and condenser sections. Semi circular channels for the placement of the copper tubing were machined to a depth of 3.175 mm in the copper plates in order to increase the contact area between the copper tubing and the copper plates. In order to meet the goal for this OHP of increasing the time that liquid spends in the evaporator some of the turns for the tubing would have to only occur in the evaporator. This resulted in a heat pipe with 3 turns in the condenser and 6 turns in the evaporator as shown in Fig.2.1.

After machining the copper blocks were cleaned with a 50/50 solution of Duraclean and water, and rinsed with water. The solution removes oxidation and machining oils from the copper plates. The copper tubing is then inlaid into the channels along with a layer of Omegatherm 201 thermal paste. The ends of the copper tubing were connected using a 6.35 mm diameter copper connector with a 1.59 mm diameter charging tube. The OHP was charged using back-filling method [11]. For this study high performance liquid chromatography grade water was used as the working fluid. After charging the heat pipe, the charging tube was sealed using pneumatic tubing crimpers and then quickly submerged in solder to guarantee a hermetic seal.

The filling ratio is defined as the liquid volume charged to the system is divided by the total volume of the channels. The previous results [4, 6, 7] show that when the filling ratio ranges from 30% to 80%, the oscillating heat pipe can function well. Filling ratios of about 50% and 70% were used in the current investigation. This heat pipe was charged with a 70% fill ratio for testing.



Fig. 2.1 oscillating heat pipe

The second unit as shown in Figs. 2.2 and 2.3 was designed to overcome the difficulties found in the initial prototype. The first design did not have enough turns to operate efficiently at high heat flux. Therefore a much larger system was designed that would have 14 complete turns and 6 that would only occur in the evaporator. Utilizing

the bend radius of the chosen tubing, the diameter of the tubing, along with the desire for a high number of turns the size of the evaporator and condenser sections are calculated.

The turn number plays a significant role in the operation of an oscillating heat pipe. How efficiently a heat pipe operates is driven by the number turns. The number of turns also determines how well a heat pipe will operate in various positions. More turns are required for horizontal operation and for situations where the condenser is below the evaporator. The increased number of turns allows the heat pipe to overcome the effect of gravity on the liquid plugs. It was also believed that this design would be able to work against gravity in the inverted position with the evaporator above the condenser. Previous OHPs with fewer than 6 turns have only been able to work in a vertical orientation with the condenser above the evaporator. This design should work continue to work in the inverted orientation because fluid will be trapped in the extra turns of the evaporator generating the pressure required to pump fluid back to the evaporator from the condenser. Typical designs would dry out from the inability to simultaneously displace the vapor from the evaporator after expansion and overcome the effects of gravity allowing fluid to return from the condenser.

Due to the increased size required by the additional turns the new unit had dimensions for the condenser section $536.5750 \times 119.9896 \times 6.35 \text{ mm}^3$, for the evaporator section $536.5750 \times 109.9820 \times 6.35 \text{ mm}^3$; and the adiabatic region was 70 mm long. A new cooling block for the system also had to be manufactured. It was determined that a design with each side of the block being independently supplied with cooling fluid would be best. The cooling block was attached to the system using 8-32 thread 18-8 stainless steel socket cap screws. To attach the two copper plates to each

other two connectors were manufactured from 6.35mm by 6.35mm stainless steel rod stock with holes machined to match up with holes for the condenser block. The heat pipe was charged with a filling ratio of 70% (14.7 ml), and 50% (10.2 ml) respectively.

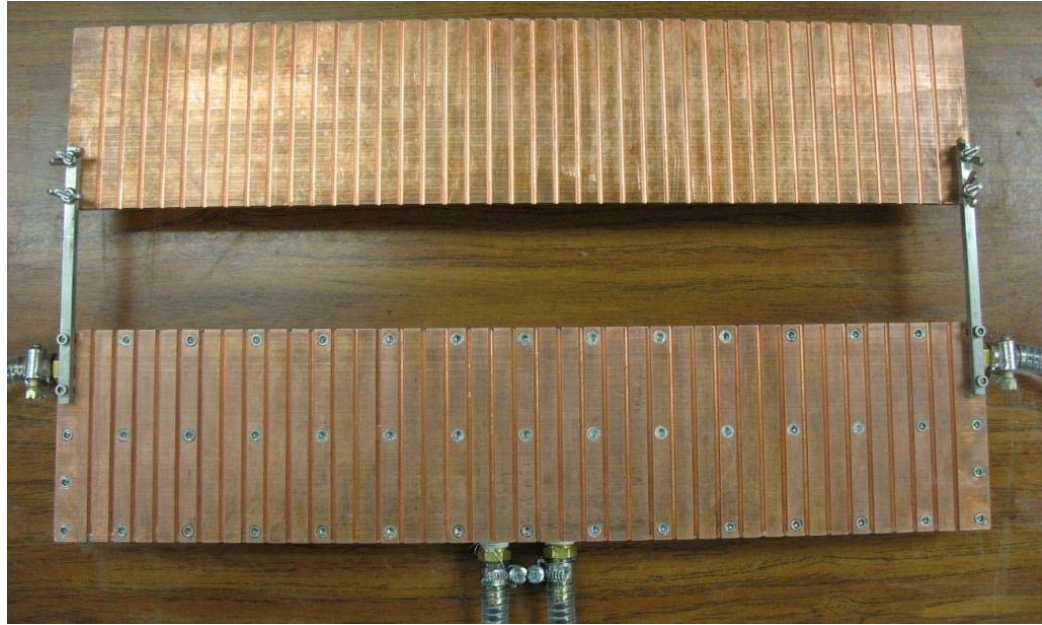


Fig 2.2 Cooling and heating blocks for Uneven Turns OHP during assembly

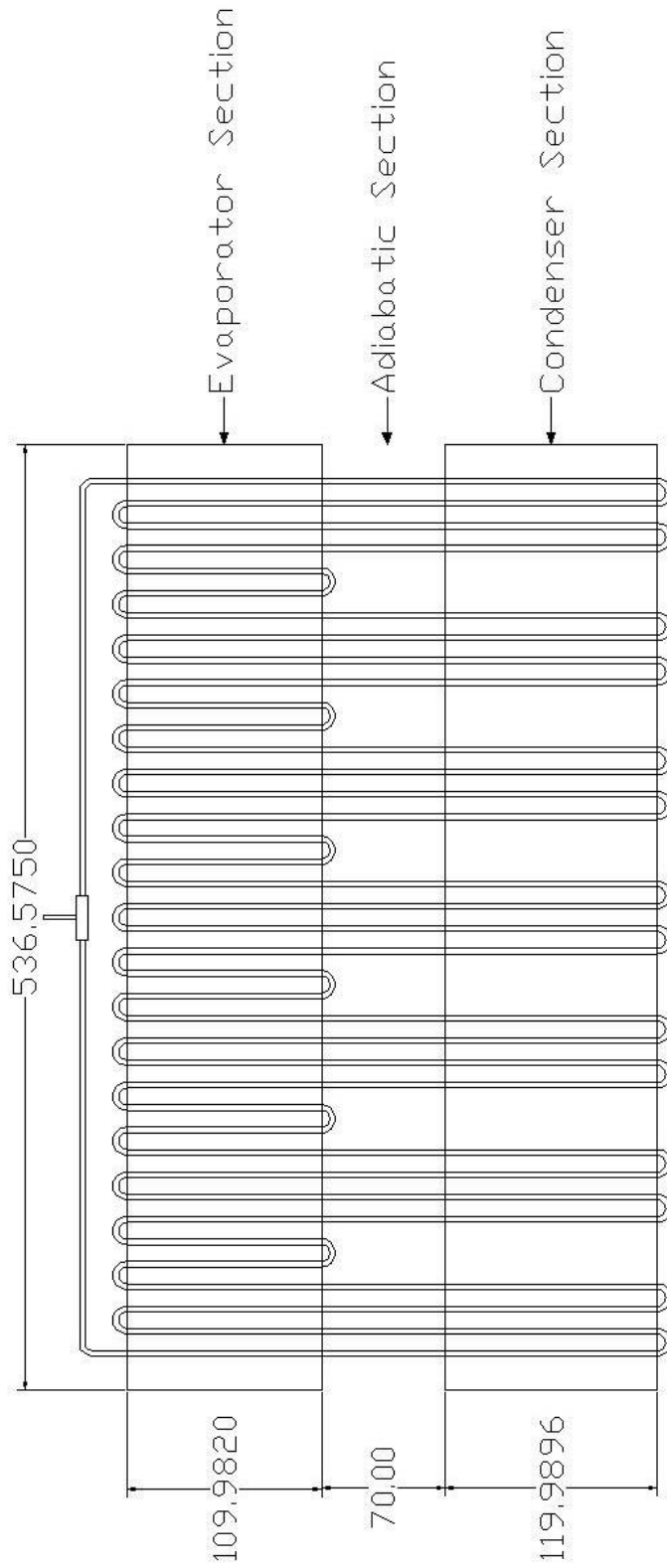


Fig 2.3 Uneven Turns OHP schematic design



Fig. 2.4 Prototype II after assembly

Chapter 3

Experimental Setup and Procedure

Setup Overview

The OHPs were tested using the experimental setup illustrated in Figure 3.1. This consists of a test section, a NI SCXI-1600 data acquisition system, a personal computer, a Julabo F 25 - ED water chiller and circulator, a Statco voltage regulator, and a Fluke 45 multimeter. A flat plate heater was attached to the evaporator and an aluminum cooling block was attached to the condenser. T type thermocouples were attached to the heat pipe. The heat pipe was then insulated with fiber glass insulation.

The type T thermocouples used for the experiment have a variation of $\pm 0.25^{\circ}C$. There is some additional uncertainty in the measured temperature for the incoming and outgoing fluid due to movement of the thermocouples in the fluid path. There was also some variation in the performance of the circulating baths at maintaining temperature. The variation is due to the use of multiple cooling baths with different control systems for maintaining fluid temperature. The system during testing had an average energy loss of 12.5% to the surrounding environment.

Condenser Section

Testing of the heat pipe was done in a controlled manner utilizing a Julabo F 25 - ED water chiller and circulator with $\pm 0.1^{\circ}C$ precision. The temperature of the bath was maintained at a given temperature. From the chilled water bath, the water flowed through

water lines to the condenser block. The condenser block two channels were drilled through the width of the block and then threaded to allow chilled water to flow through the block. Standard barbed hose fitting were attached to the block and then connected to the water lines for the chilled water bath.

Evaporator Section

To simulate a heat source a 152.4 mm long by 38.1 mm wide 400 watt 120 volt heater was attached using clamps to the evaporator. Omega Therm “201” thermal paste was used to make sure that there was good thermal conductivity between the heater and the evaporator.

The power output of the heater was determined by measuring the resistance of the heater and the voltage input by the Statco voltage regulator. The power output by the heater can be calculated using Eq. (3.1) where P is power, V is voltage, and R is resistance. Voltage and resistance were recorded directly from a fluke multimeter that was connected to the heater.

$$P = \frac{V^2}{R} \tag{3.1}$$

Because prototype I is much smaller than the prototype II, the power level for two the prototypes is different. Therefore during the testing of prototype I, the power was incremented from 20 watts through 50 watts and in increments of 10 watts. For prototype II, the power was incremented from 100 watts through 1200 watts and in increments of 100 watts. At each increment the system was allowed to reach steady state

before data was captured. Testing was done with the cooling bath set at a given temperature.

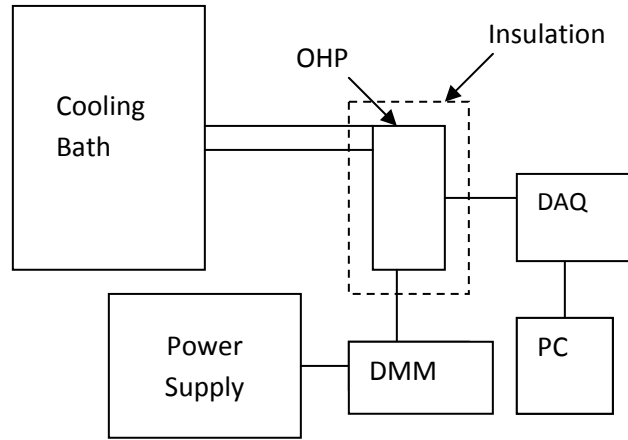


Fig. 3.1 Experimental Setup

Chapter 4

Results and Discussion

Prototype I

Utilizing the experimental setup and procedure described above, the effects of the power input and condenser temperature on the heat transfer performance of OHP were studied. The condenser water was set at 20°C . The heat load was varied between 20 watts and 50 watts. The heat pipe was tested with a filling ratio of 70%. As shown when in Figure 4.1 as thermal load was increased on the heat pipe with the condenser set at 20°C the temperature difference between the evaporator and the condenser increases to a peak of 76°C at 40 watts. The heat transfer performance is not what was expected.

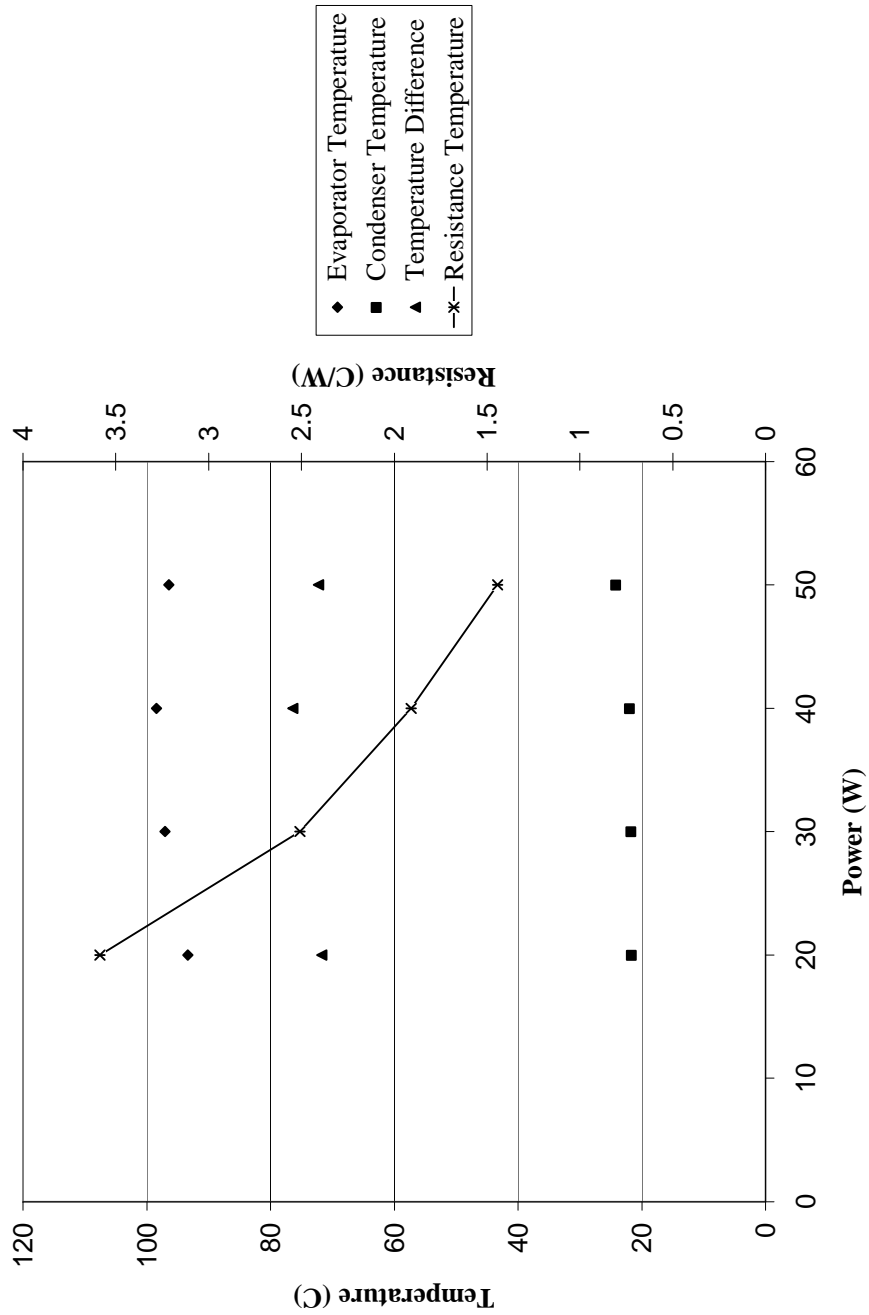


Fig. 4.1 Power input effect on the heat transfer performance in an OHP and the thermal resistance of the OHP (cooling bath temperature = 20 °C, a filling ratio =70%, and tilted angle = 90 degrees)

Thermal resistance is defined as:

$$R = \frac{T_e - T_c}{Q} \quad (4.1)$$

where T_e is the temperature of the evaporator, T_c is the condenser temperature, and Q is the heat input. With the condenser supply temperatures set to 20°C , the heat pipe had a resistance of $1.44^\circ\text{C}/\text{Watts}$ at 50 watts, which is much worse than the typical OHP.

Prototype II

The heat pipe was tested using a similar test setup to Prototype I with a few changes. The second design required the use of two Julabo circulator cooling baths to maintain the temperature of the condenser water supply; a Julabo F34 and a Julabo FP40 were used. Each cooling bath was attached to one side of the cooling block. This was necessary to prevent one side of the system from receiving greater cooling than the other. Standard barbed hose fitting were attached to the block and then connected to the water lines for the chilled water baths using quick disconnect fittings. Two flat plate heaters were attached to the evaporator. Two 600 watt strip heaters wired in series and attached to the evaporator section with Omegatherm 201 paste used to decrease the contact resistance. A Fluke 175 DMM was used to measure the voltage and the resistance. During testing the power was incremented from 100 watts through 1200 watts with increments of 100 watts. This OHP was attached to an aluminum test stand manufactured from 80/20. This was done so that the system could be tested in three positions, vertical (90 degrees) with condenser above the evaporator, horizontal (0) with the condenser and the evaporator parallel in the horizontal plane, and finally inverted (-90) with the condenser below the

evaporator. The OHP was tested using the configurations described in Table 4.1 at power inputs varying from 100 watts to 1200 watts in increments of 100 watts. The system was also compared for startup response with the data acquisition system recording the rise from initial temperature to operating conditions with the heaters set to 100 watts.

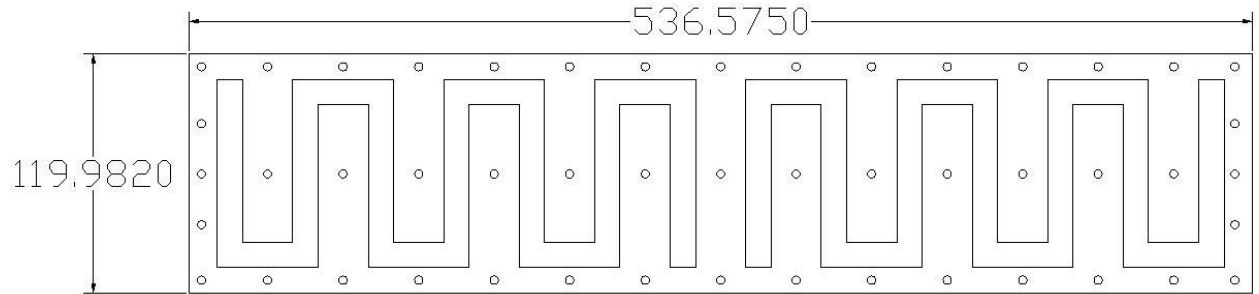


Figure 4.2 Aluminum condenser block (mm)

Table 4.1 Test Configurations

		Filling Ratio			
		70%		50%	
Cooling bath Temperature (C)	Orientation				
	40	-90	0	90	-90
60	-90	0	90	-90	
80	-90	0	90	-90	

Results

The system was tested with experimental setup and procedure previously described to find the effects of the power input, condenser temperature, filling ratio, and tilted angle on the heat transfer performance in OHPs. Figures 4.3, 4.4, 4.5 show the experimental results of input power effect on the evaporator and condenser temperatures including the transient process. As shown in Figures 4.4-4.6, the system on startup is remarkably consistent in that it starts to reach steady state with a temperature between 100°C and 115°C . In Figure 4.3 it can be seen that the system reaches steady state much faster in the 90° position than in the other two positions; in addition it can be seen that the temperature difference is 10°C less in this position. While the -90° position has larger temperature oscillations than the other two positions, it oscillates much more quickly. Figure 4.4 also shows that the system reaches steady state at an earlier time in the 90° position; however, the 0° position starts to oscillate first. It can also be seen that as the orientation is changed, the temperature difference significantly decreases. From Figure 4.5, all three orientations achieve steady state in the same time period; with the 90° position showing the smallest temperature difference at 27°C .

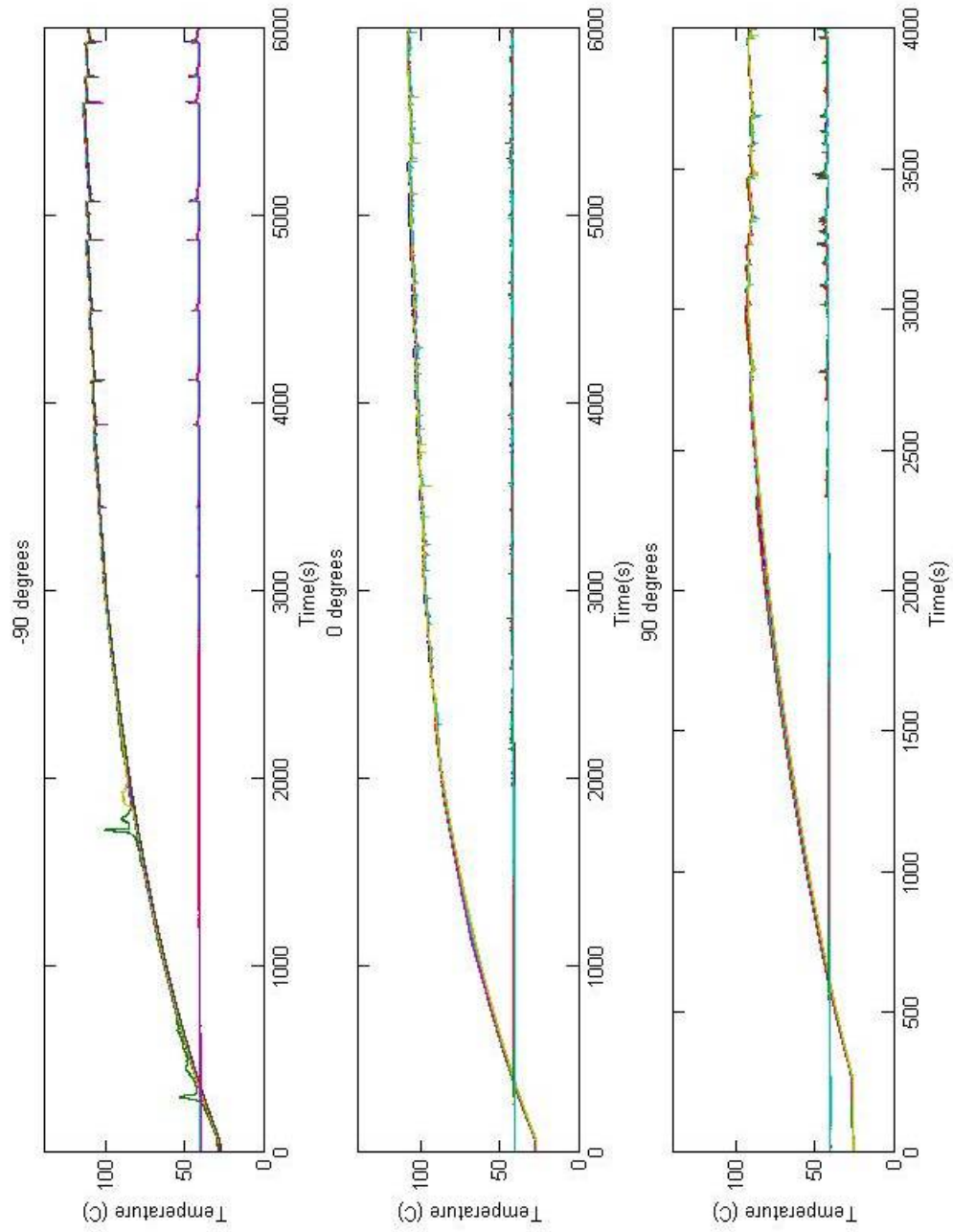


Fig 4.3 Power input effect on the heat transfer performance in an OHP (cooling bath temperature = 40 °C and a filling ratio =70%)

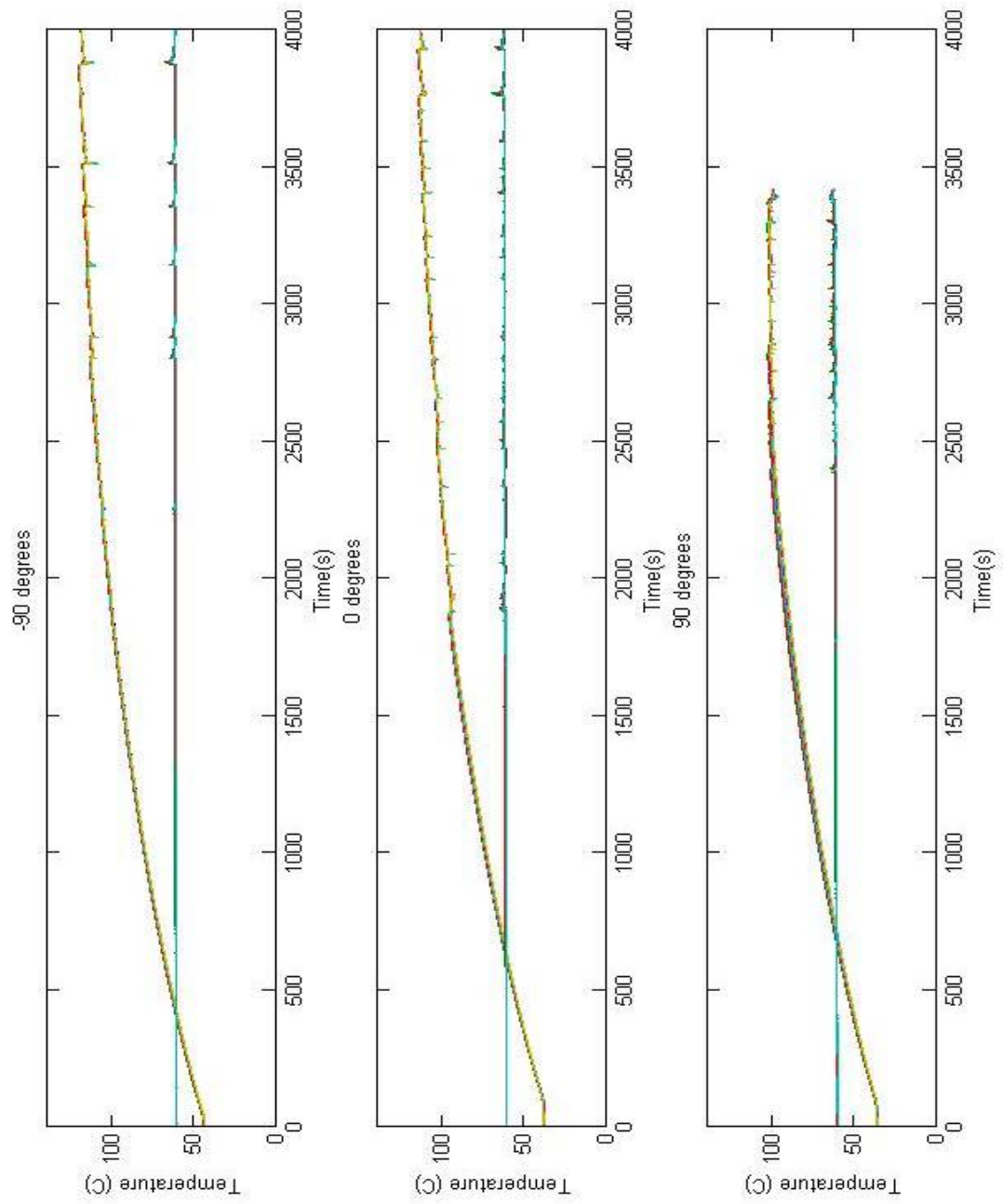


Fig 4.4 Power input effect on the heat transfer performance in an OHP (cooling bath temperature = 60 °C and a filling ratio =70%)

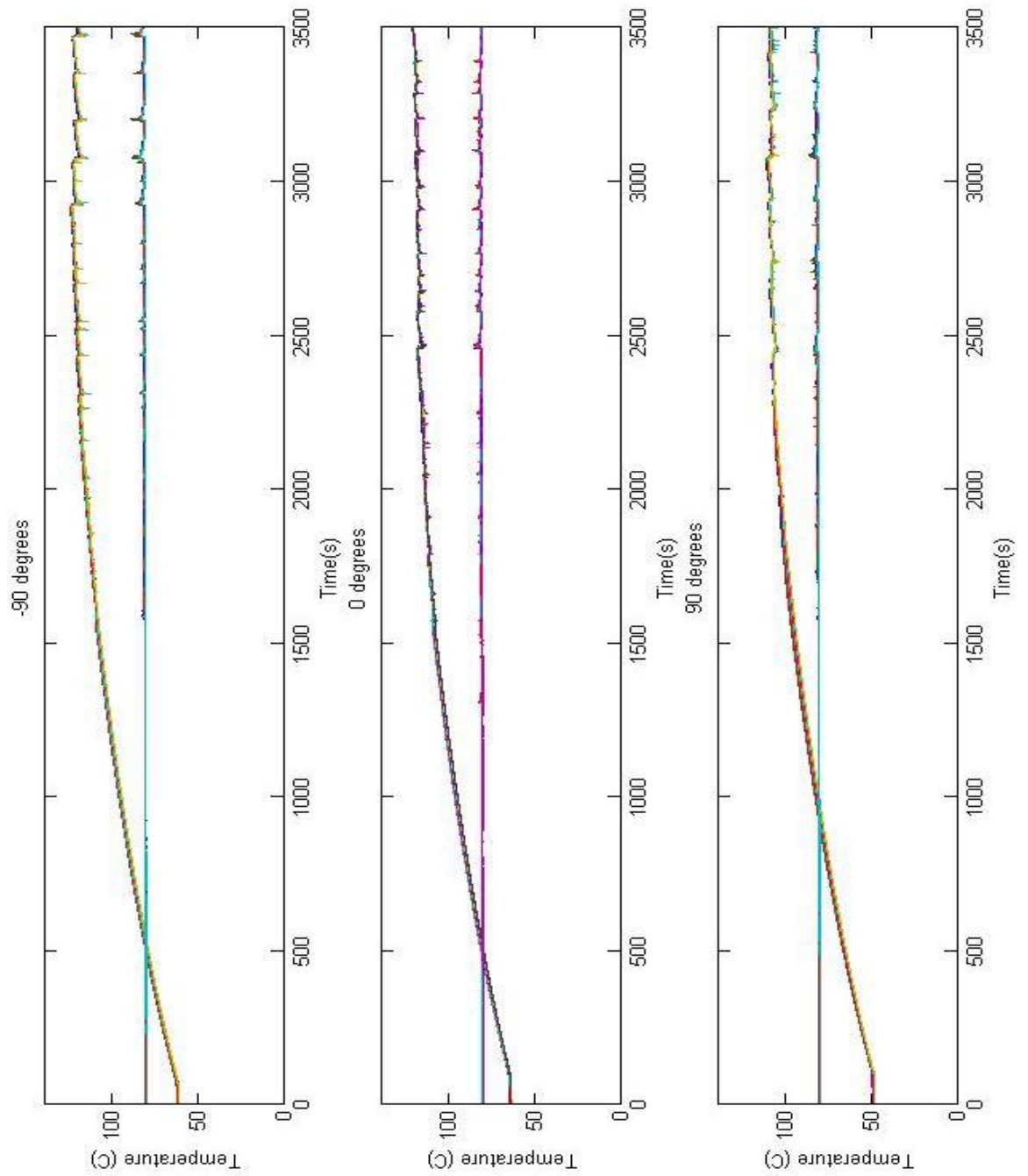


Fig 4.5 Power input effect on the heat transfer performance in an OHP (cooling bath temperature = 80 °C, a filling ratio =70%)

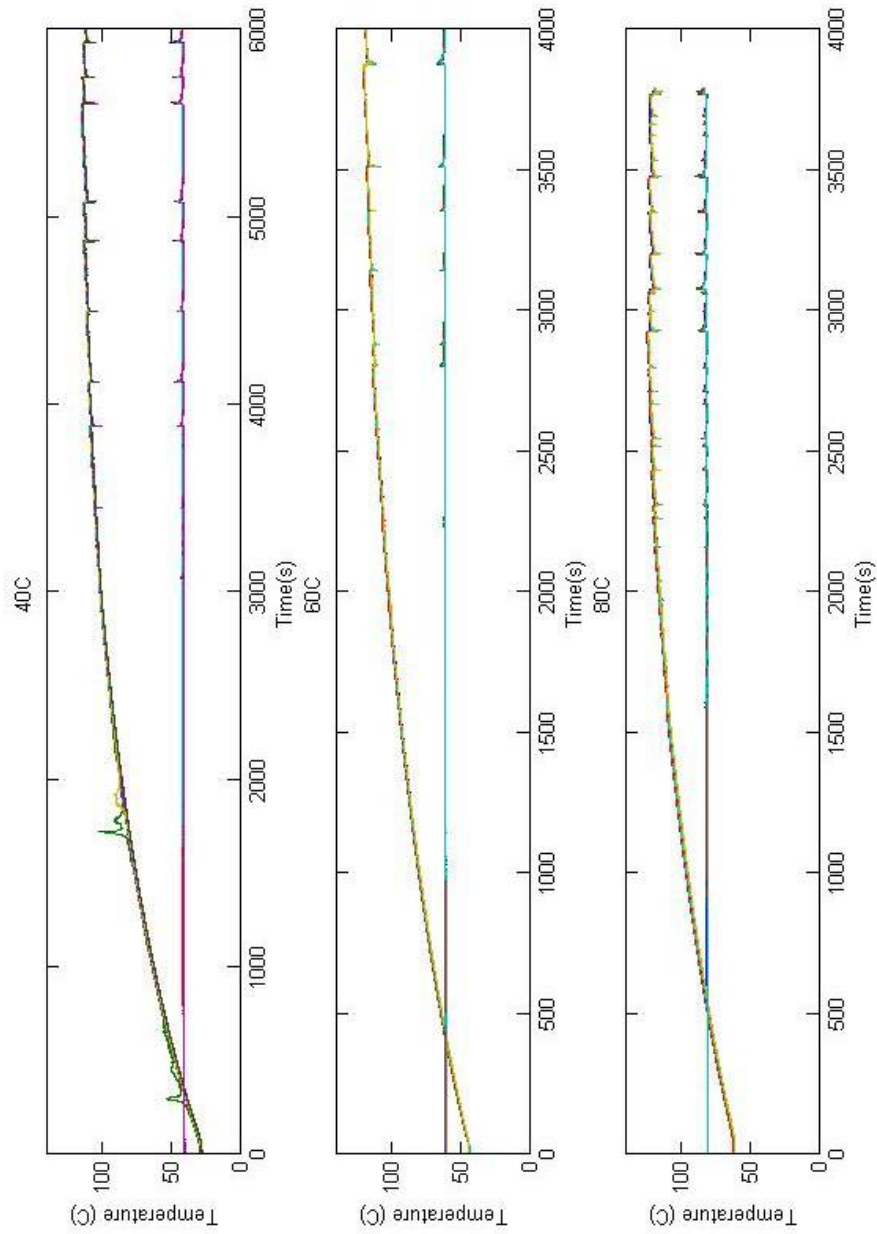


Fig 4.6 Power input effect on the heat transfer performance in an OHP (cooling bath temperature = 40, 60, and 80 °C, a filling ratio = 70%, and tilted angle = -90 degrees)

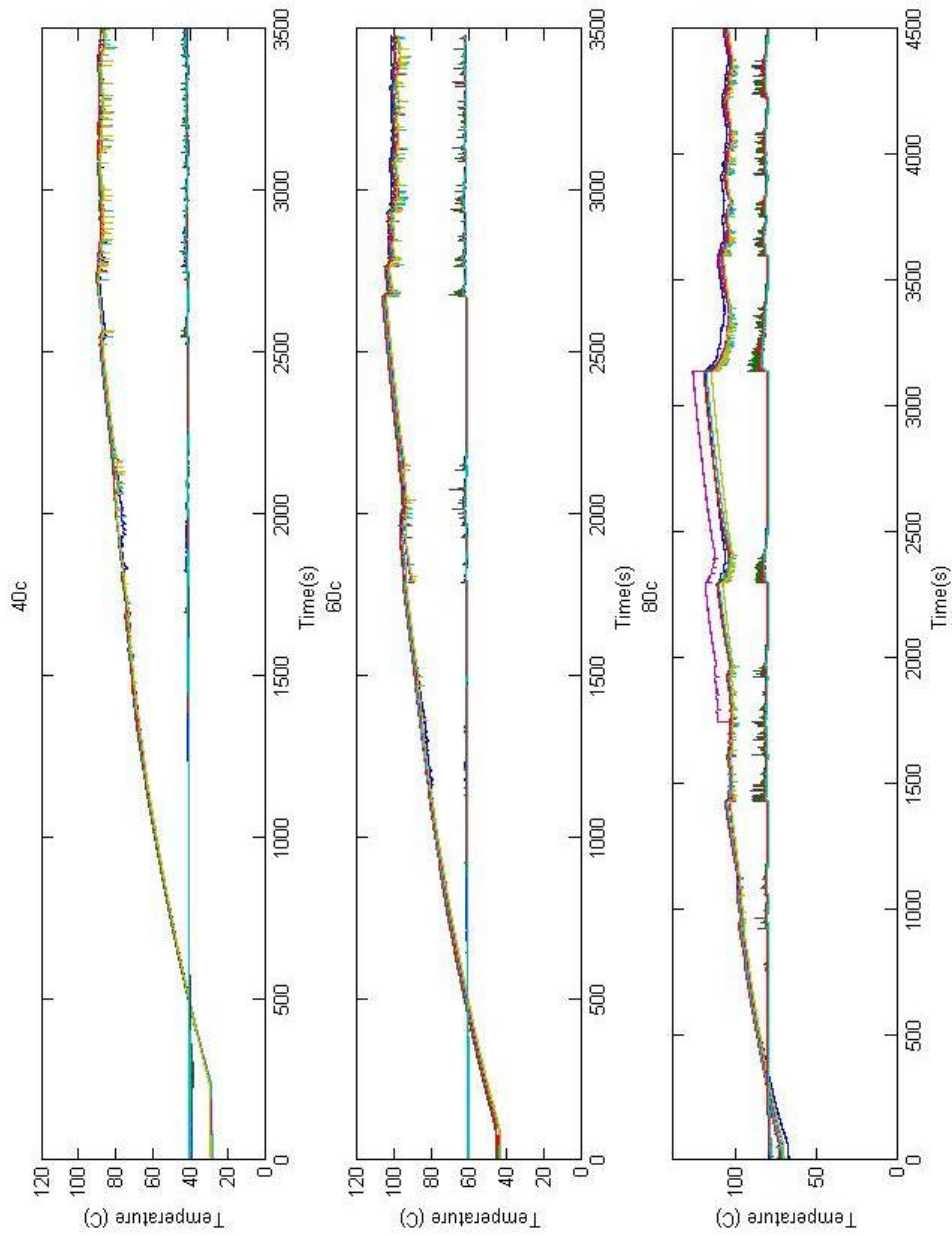


Fig 4.7 Power input effect on the heat transfer performance in an OHP (cooling bath temperature = 40, 60, and 80 °C, a filling ratio = 50%, and tilted angle = -90 degrees)

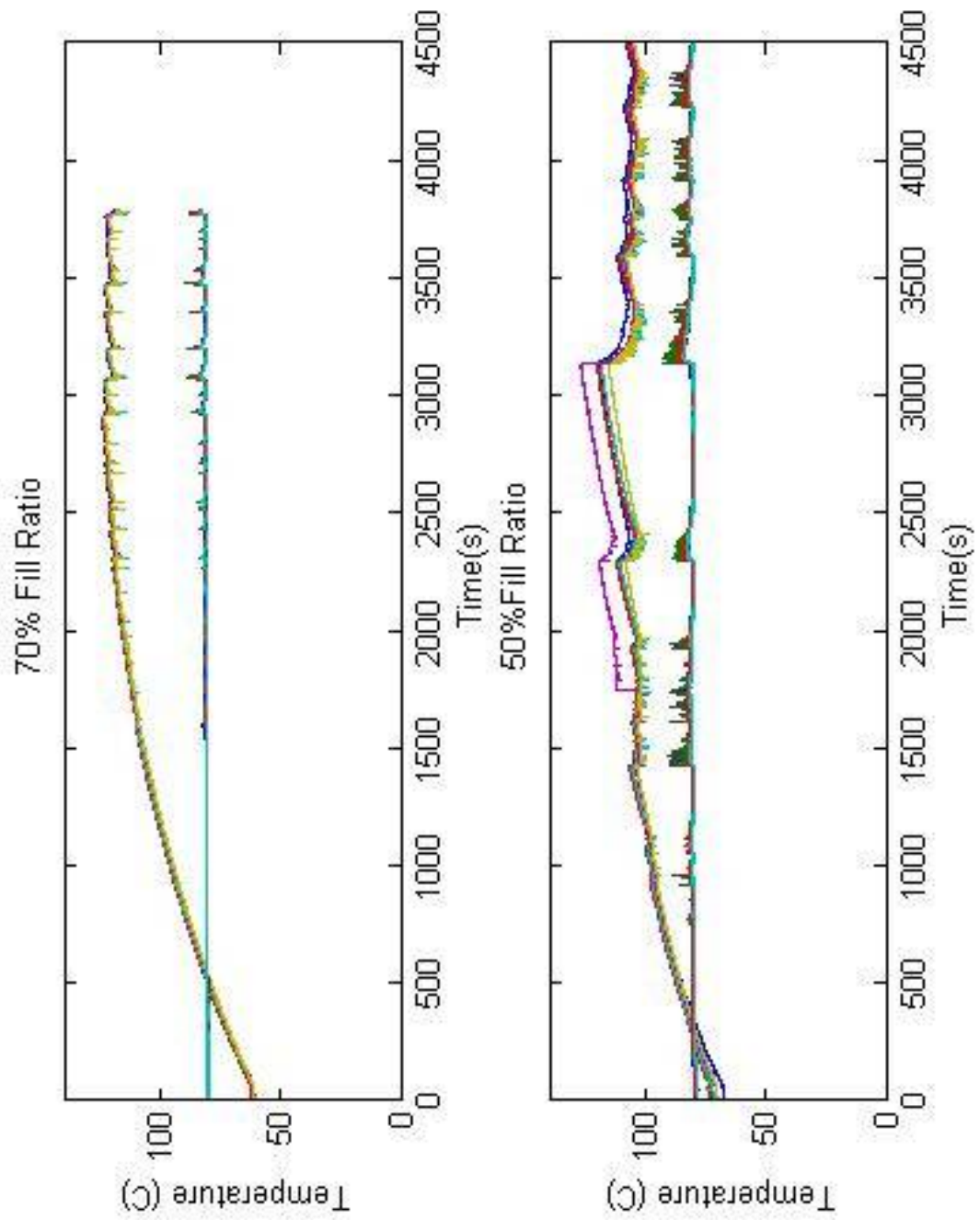


Fig 4.8 Power input effect on the heat transfer performance in an OHP (cooling bath temperature = 80 °C, a filling ratio =50% and 70%, and tilted angle = -90 degrees)

Figures 4.6-4.8 describe the experimental results of input power effect on the evaporator and condenser temperatures at the titled angle of -90 degrees, i.e., the heating section on the bottom and cooling section on the top. As shown, in figure 4.6 as the cooling bath temperature is increased the temperature difference stays the same at 50°C for cooling bath temperatures 40°C and 60°C; however there is a significant decrease once the cooling bath temperature is raised to 80°C at which point the temperature difference falls to 38°C. As can be seen in Figure 4.7 the OHP with a 50% fill ratio, in the inverted position, with an 80°C cooling bath temperature over shoots to 130°C before settling near 115°C; this is possibly due to a pressure imbalance in the distribution of vapor bubbles to liquid plugs. Using figure 4.8 to comparing the start up trends between 70% fill ratio and 50% fill ratio for the inverted heat pipe with the 80°C cooling bath temperature shows that for low wattages the system has similar performance regardless of fill ratio. The system with the 50% fill ratio with cooling baths set to 80°C raised the temperature of the evaporator to the high 70s within seconds of the insulation being applied to the system. This shows that fluid was circulating through the system, with the condenser section acting as the evaporator.

Using equation 2.1 the thermal resistance for each test of the OHP was calculated. Based on the results it can be seen that as the power input into the OHP was increased the thermal resistance of the decreased. As can be seen in figure 4.9 through figure 4.17 maintains a similar performance from 100 watts to 1200 regardless of orientation. There is a decrease in evaporator temperature with the system in the 90 degree orientation at low heat input, although at high heat input the evaporator temperature rises to higher than

that found in either the inverted or horizontal positions. The system achieves its lowest thermal resistance of $0.028\text{ }^{\circ}\text{C}/\text{W}$ in the inverted position with the heat input at 1200 watts with the cooling baths set to $80\text{ }^{\circ}\text{C}$.

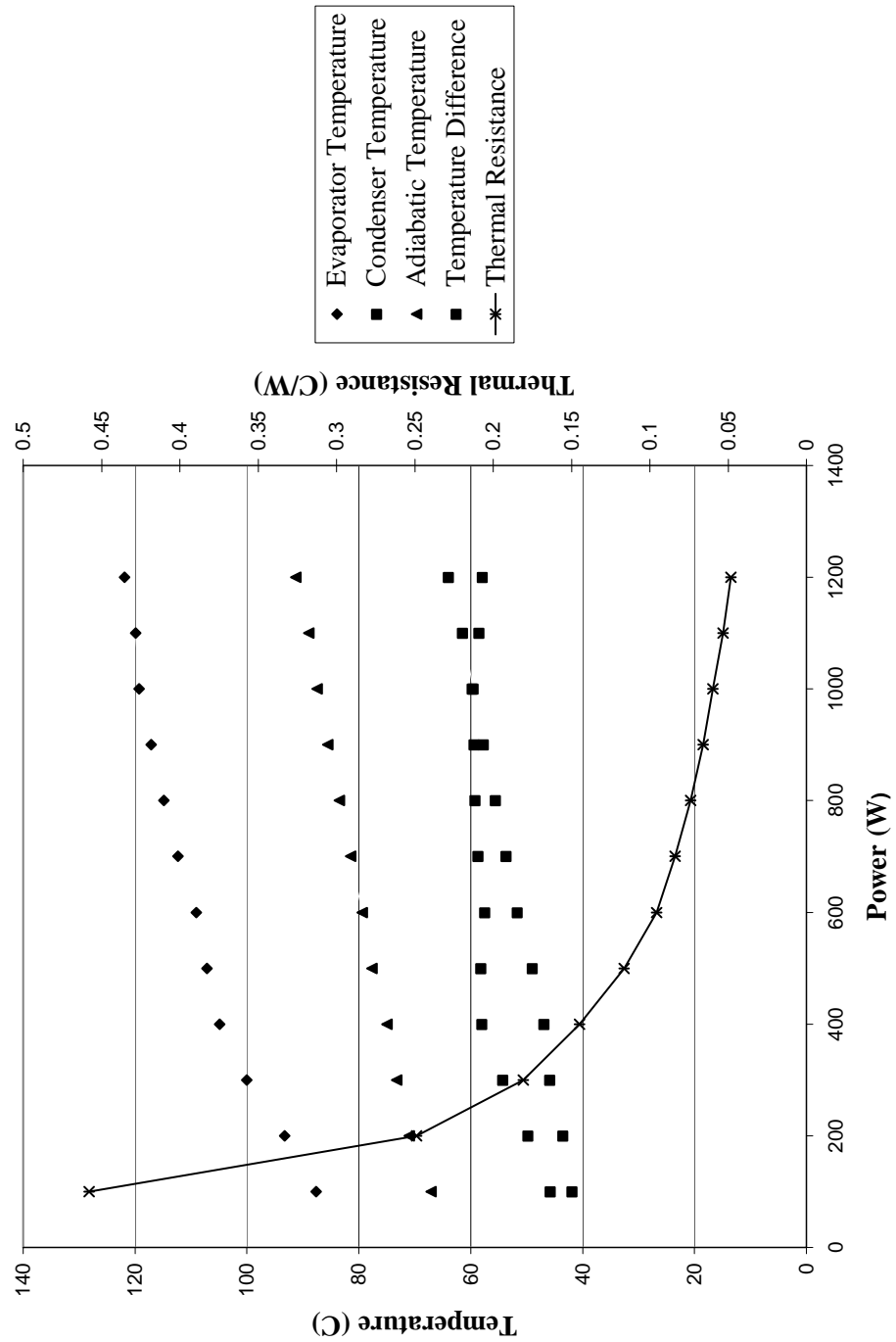


Fig 4.9 Power input effect on the heat transfer performance in the OHP and the thermal resistance of the OHP (cooling bath temperature = 40 °C, a filling ratio =50%, and tilted angle = -90 degrees)

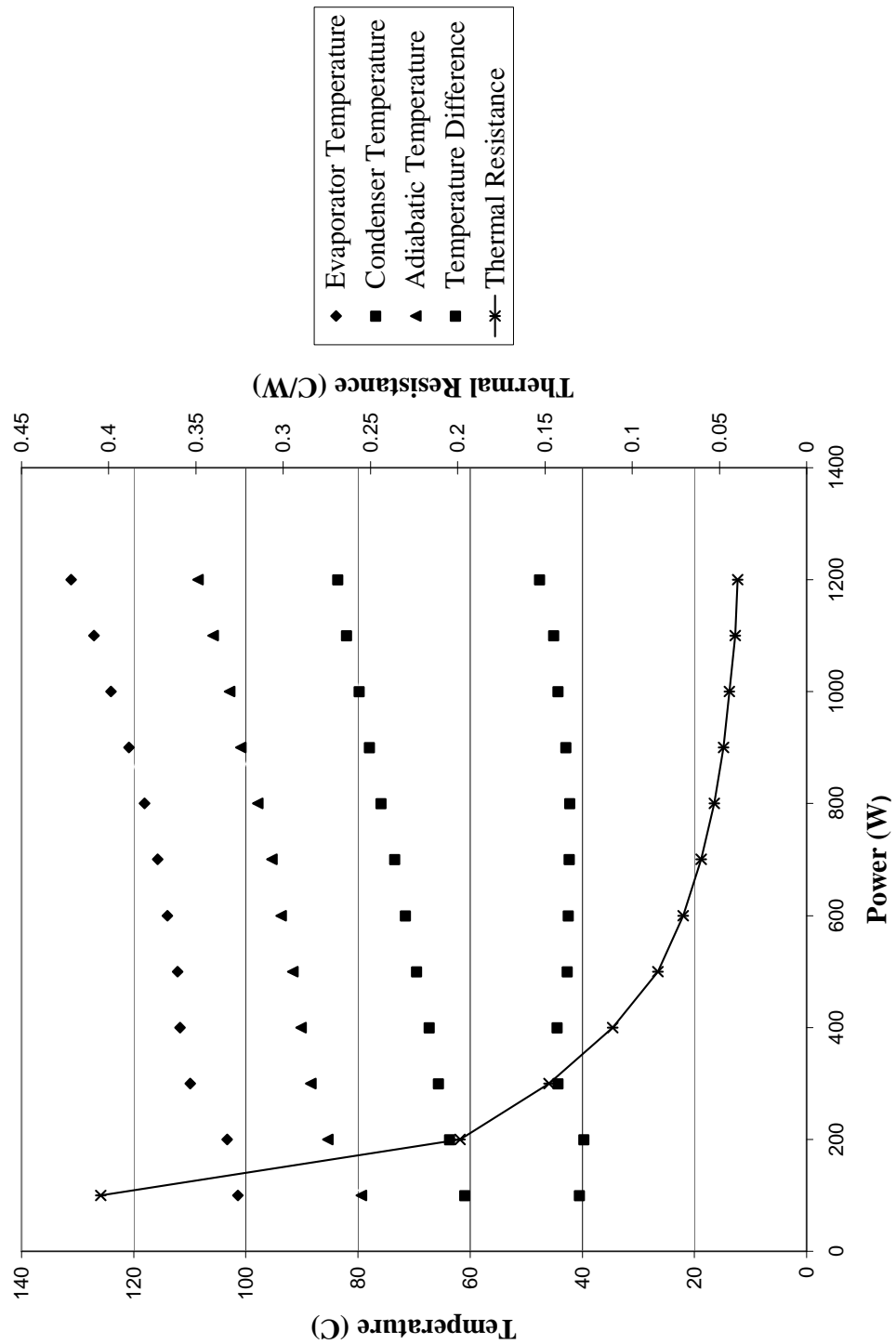


Fig 4.10 Power input effect on the heat transfer performance in the OHP and the thermal resistance of the OHP (cooling bath temperature = 60 °C, a filling ratio =50%, and tilted angle = -90 degrees)

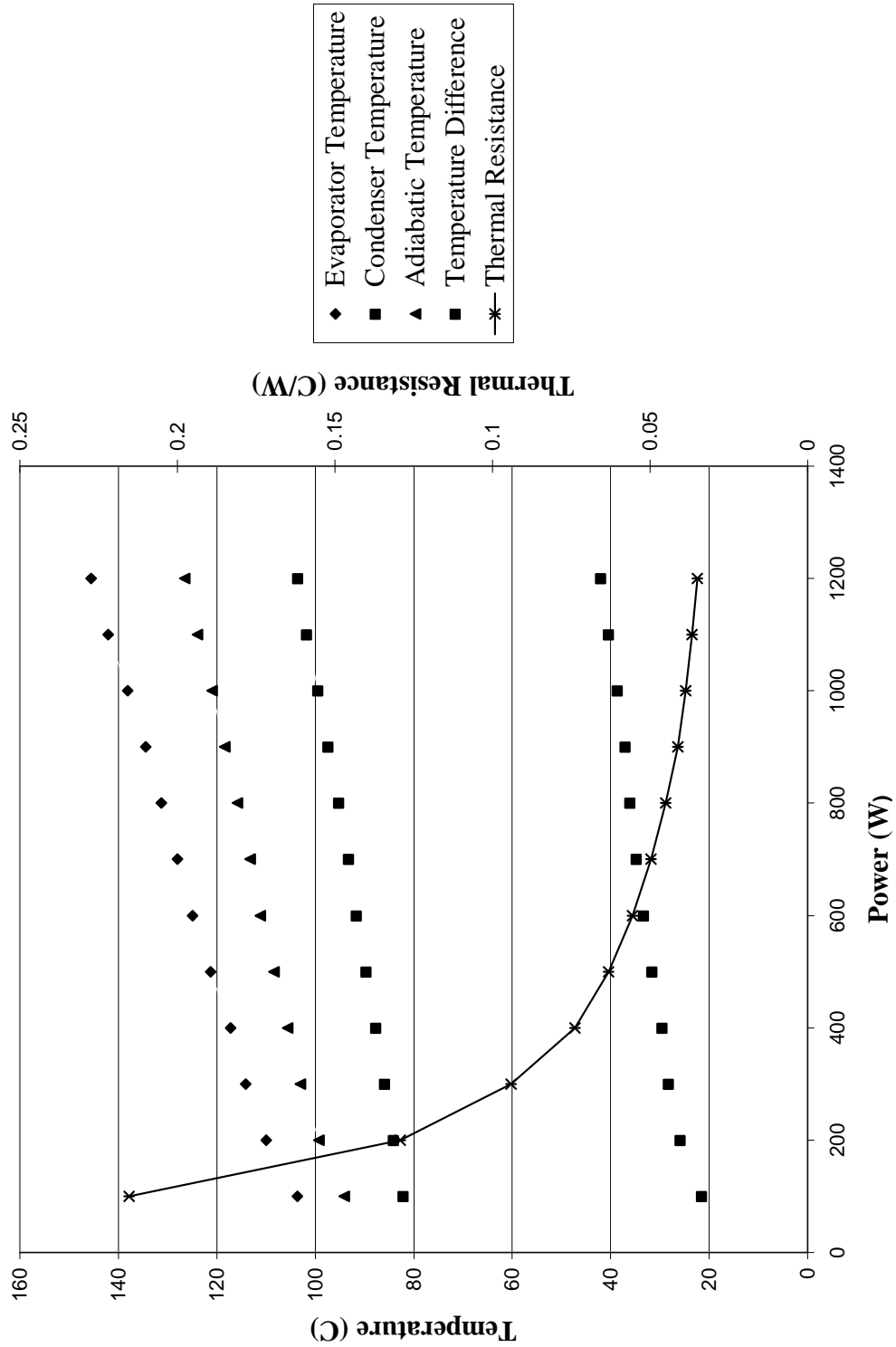


Fig 4.11 Power input effect on the heat transfer performance in the OHP and the thermal resistance of the OHP (cooling bath temperature = 80 °C, a filling ratio =50%, and tilted angle = -90 degrees)

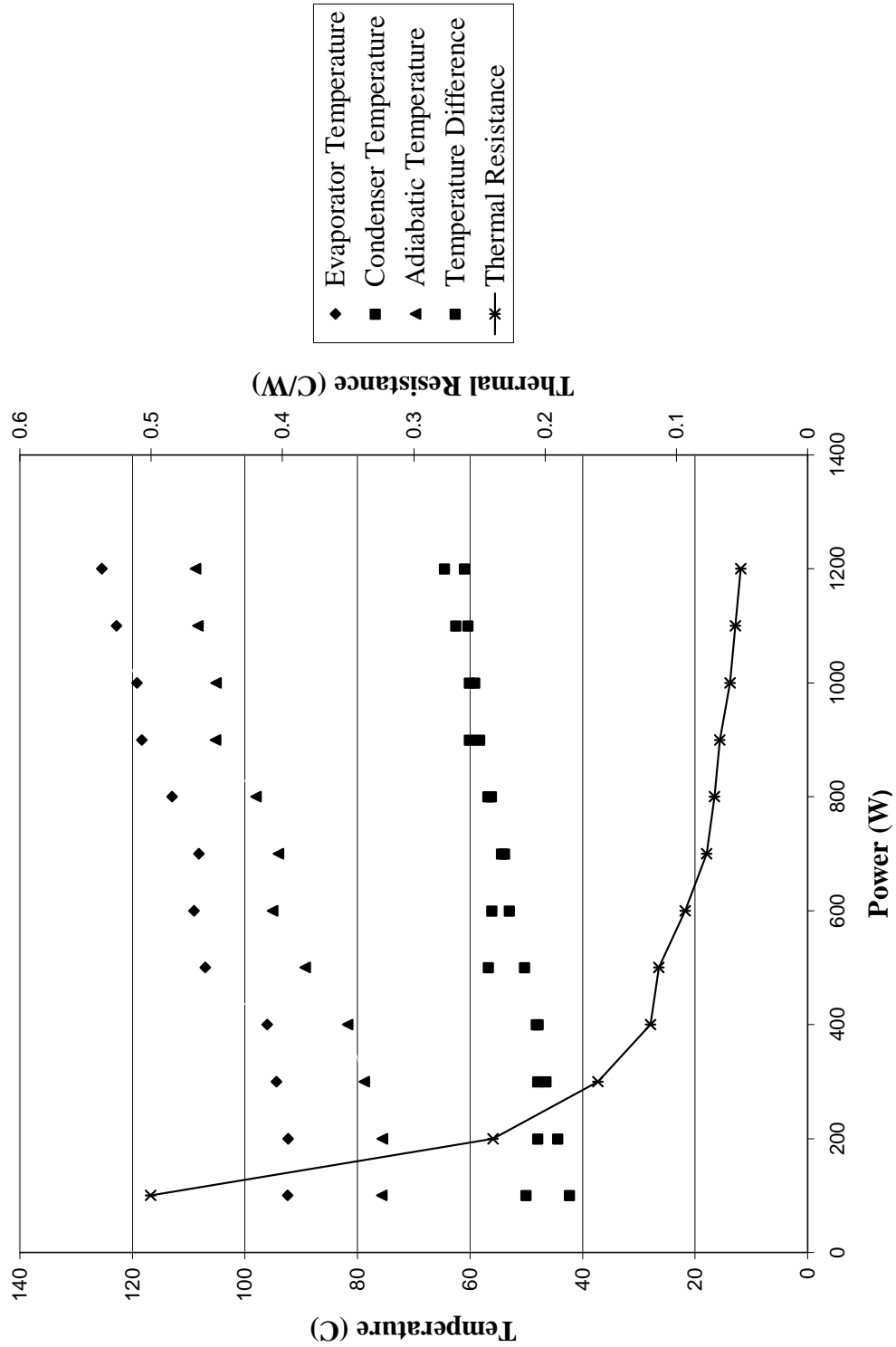


Fig 4.12 Power input effect on the heat transfer performance in the OHP and the thermal resistance of the OHP (cooling bath temperature = 40 °C, a filling ratio =70%, and tilted angle = 90 degrees)

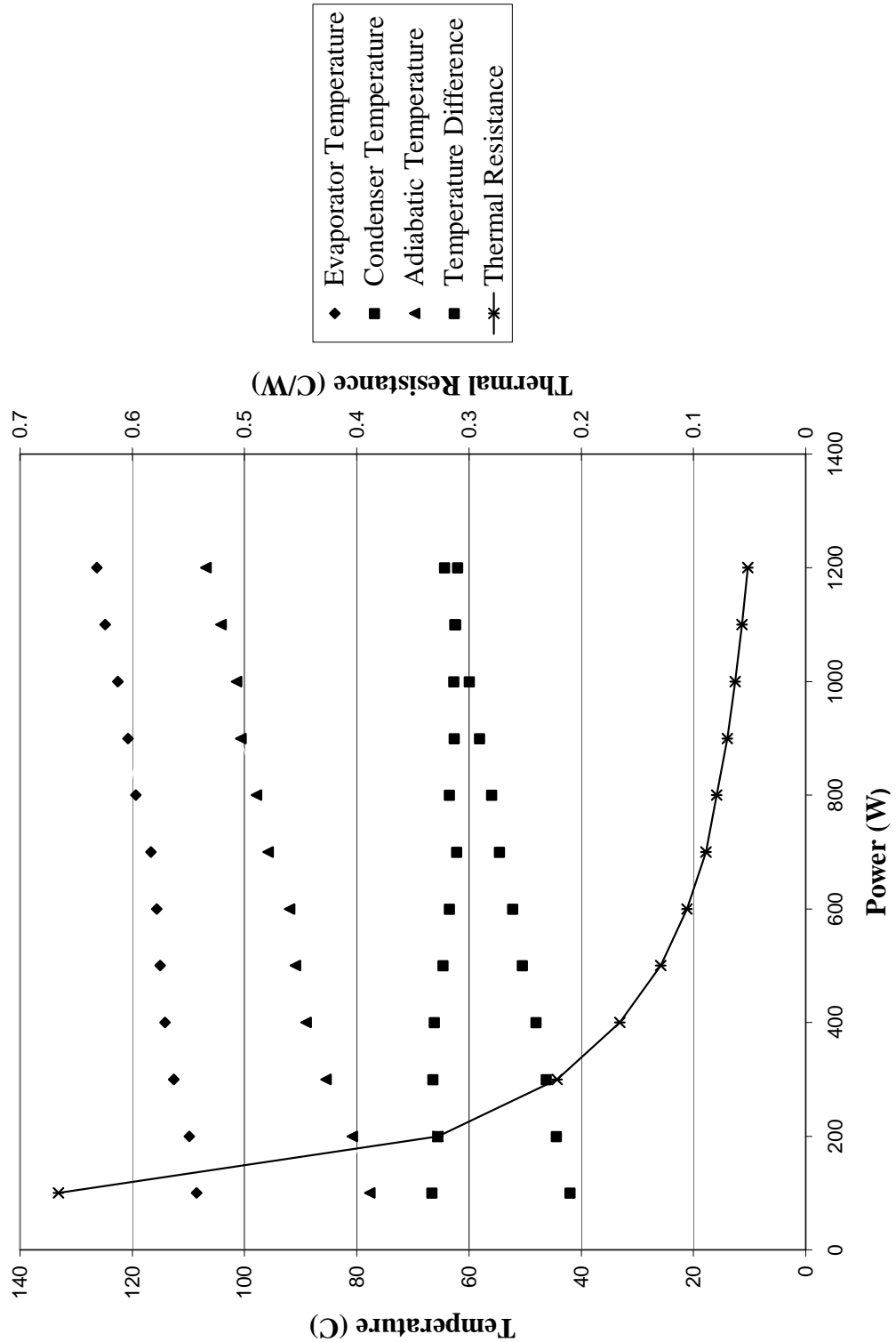


Fig 4.13 Power input effect on the heat transfer performance in the OHP and the thermal resistance of the OHP (cooling bath temperature = 40 °C, a filling ratio =70%, and tilted angle = 0 degrees)

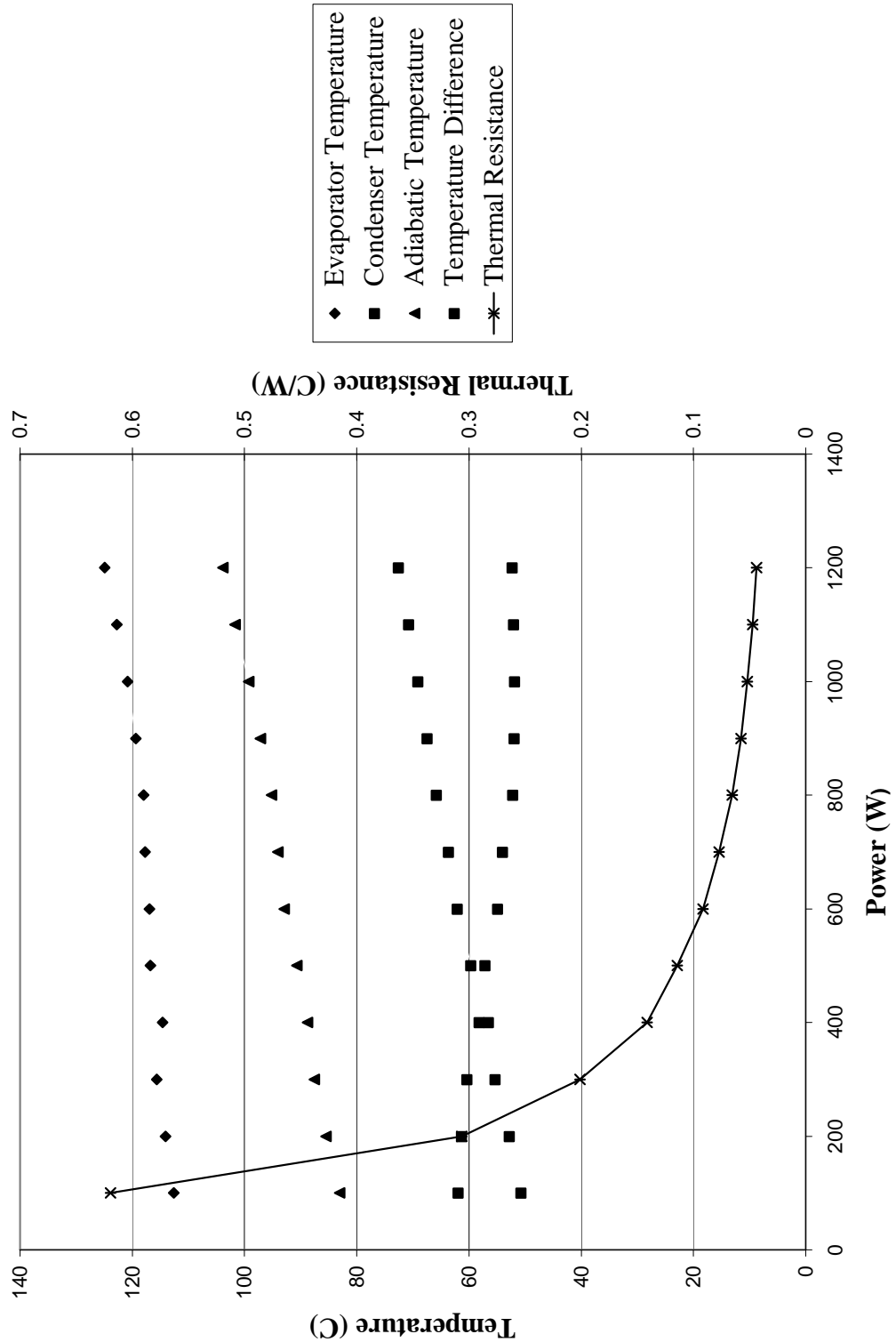


Fig 4.14 Power input effect on the heat transfer performance in the OHP and the thermal resistance of the OHP (cooling bath temperature = 40 °C, a filling ratio =70%, and tilted angle = -90 degrees)

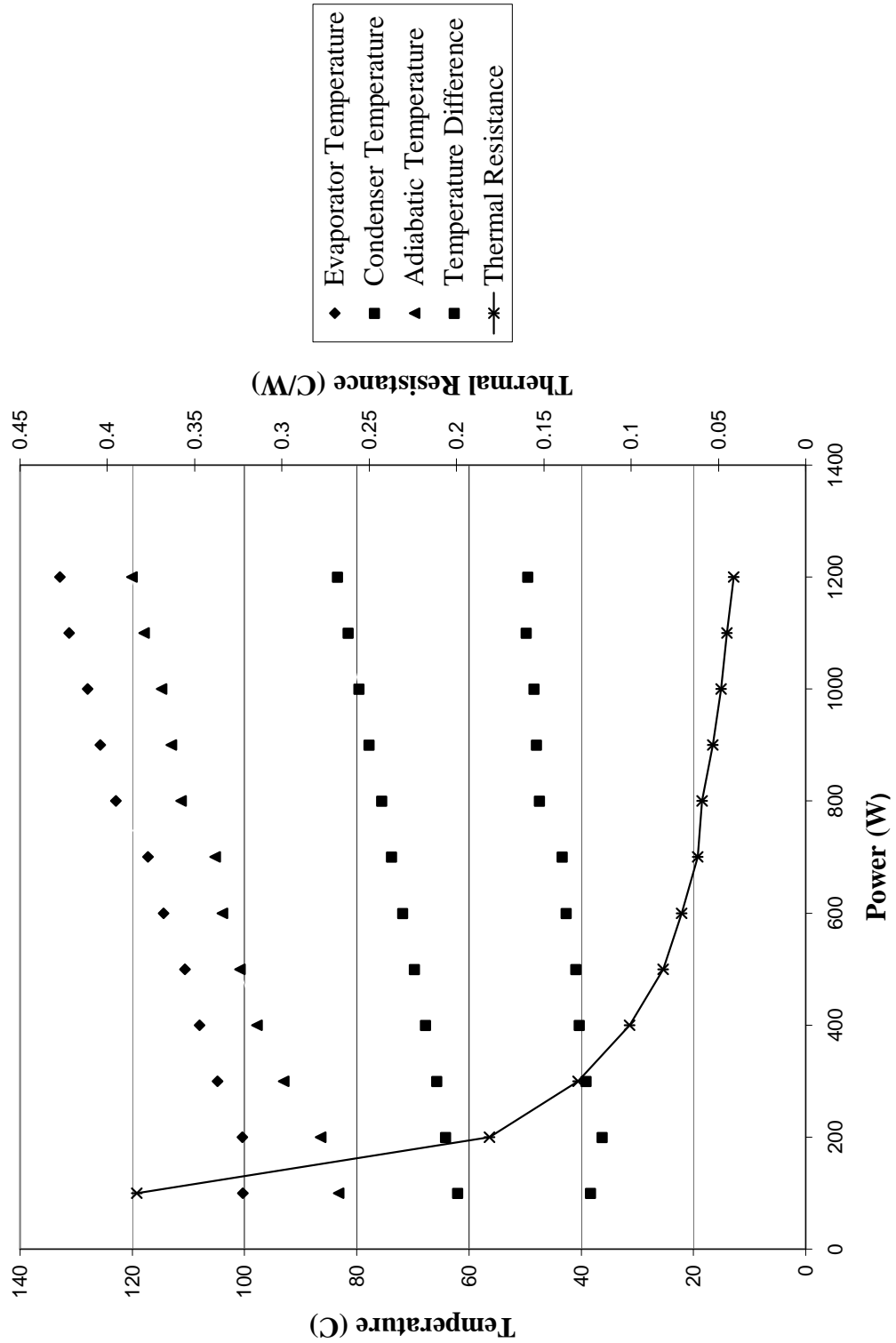


Fig 4.15 Power input effect on the heat transfer performance in the OHP and the thermal resistance of the OHP (cooling bath temperature = 60 °C, a filling ratio =70%, and tilted angle = 90 degrees)

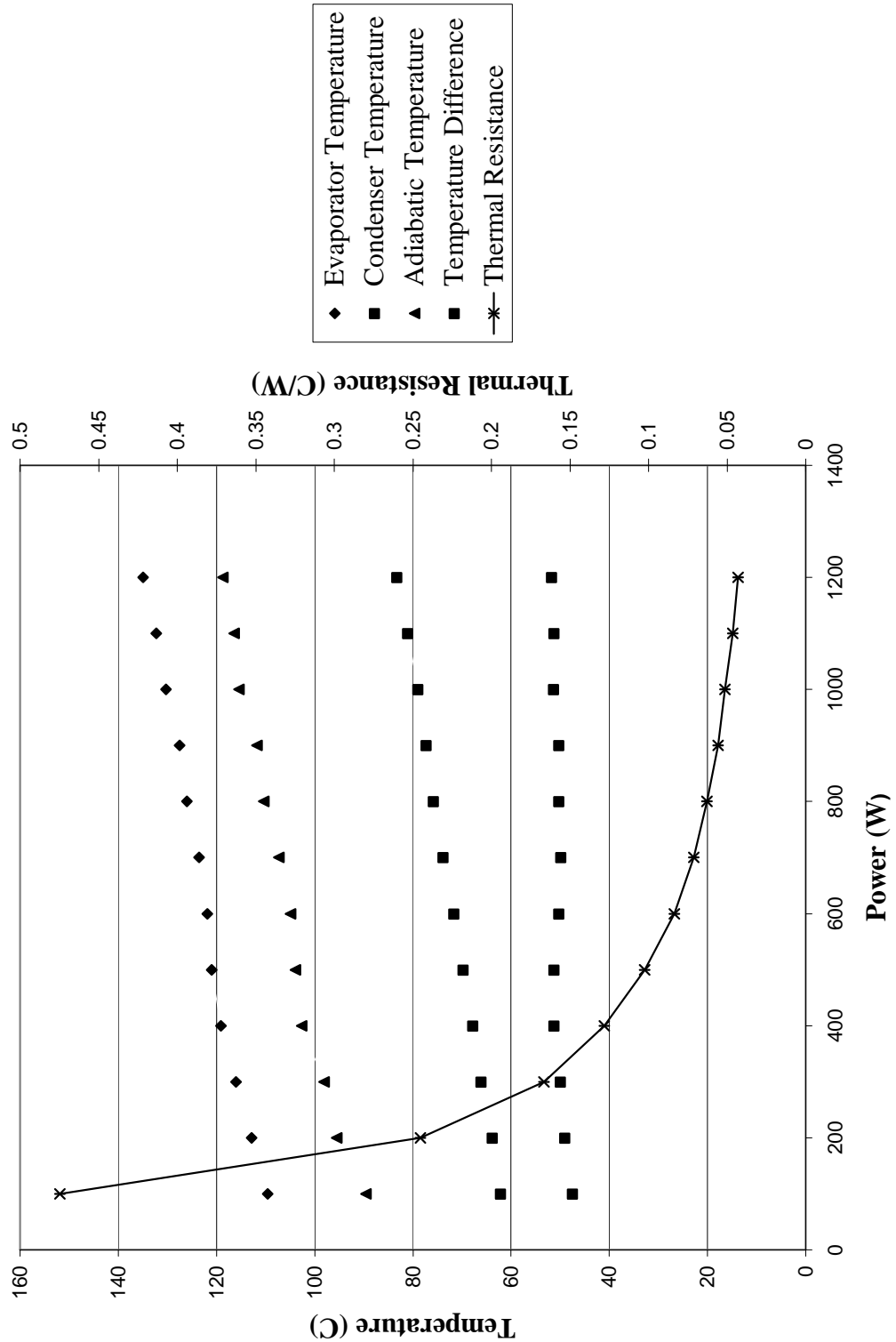


Fig 4.16 Power input effect on the heat transfer performance in the OHP and the thermal resistance of the OHP (cooling bath temperature = 60 °C, a filling ratio =70%, and tilted angle = 0 degrees)

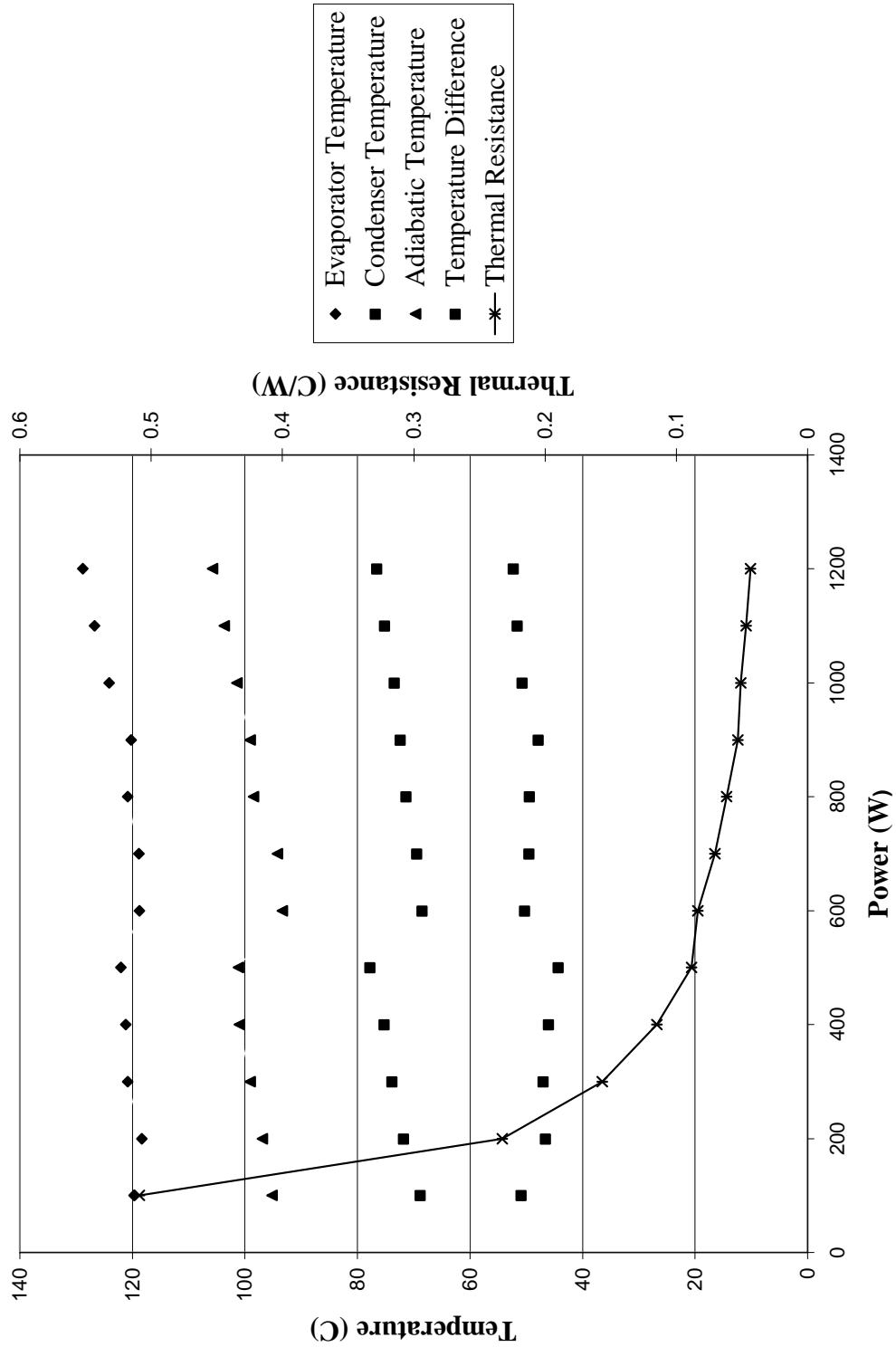


Fig 4.17 Power input effect on the heat transfer performance in the OHP and the thermal resistance of the OHP (cooling bath temperature = 60 °C, a filling ratio =70%, and tilted angle = -90 degrees)

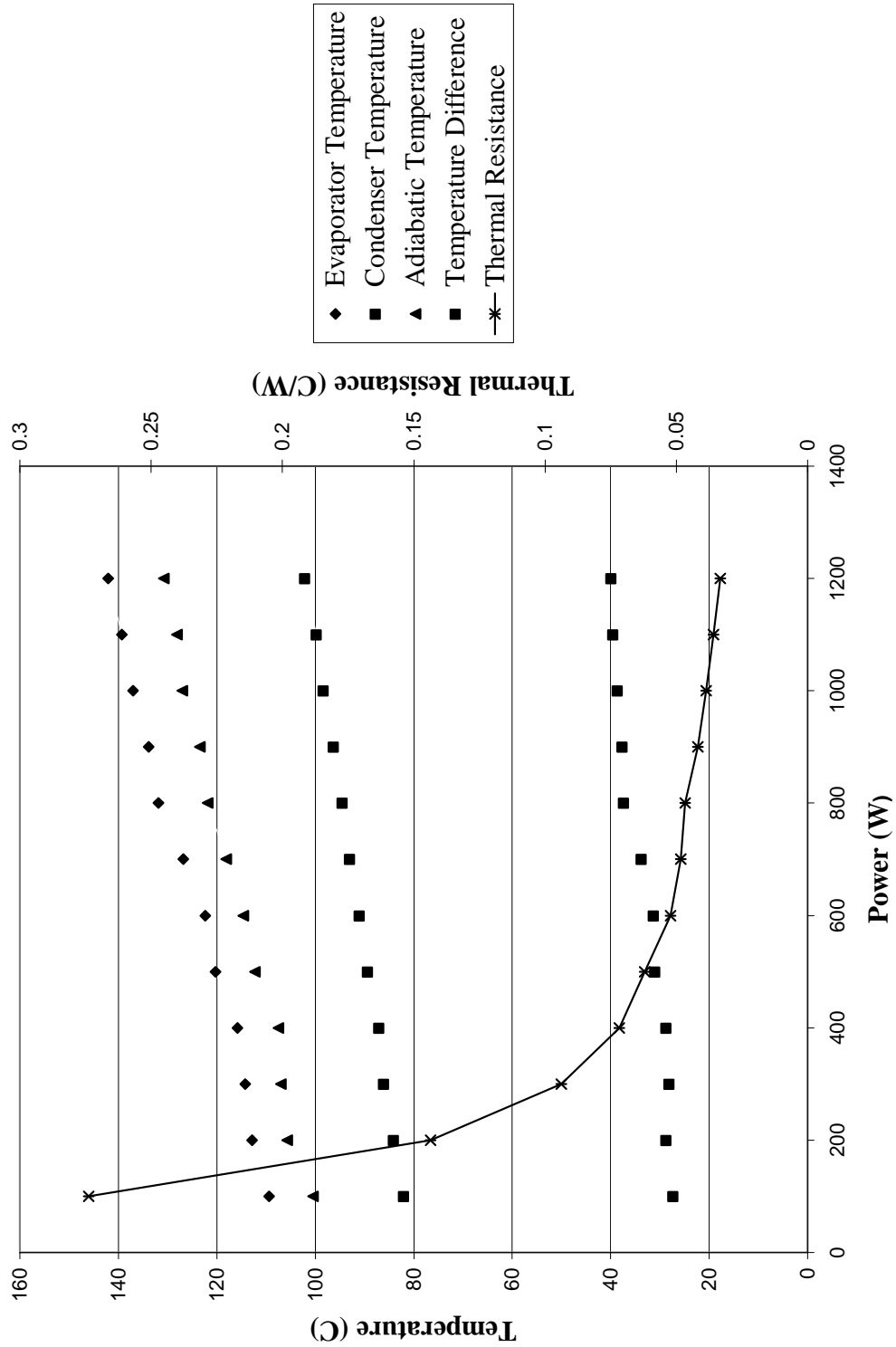


Fig 4.18 Power input effect on the heat transfer performance in the OHP and the thermal resistance of the OHP (cooling bath temperature = 80 °C, a filling ratio =70%, and tilted angle = 90 degrees)

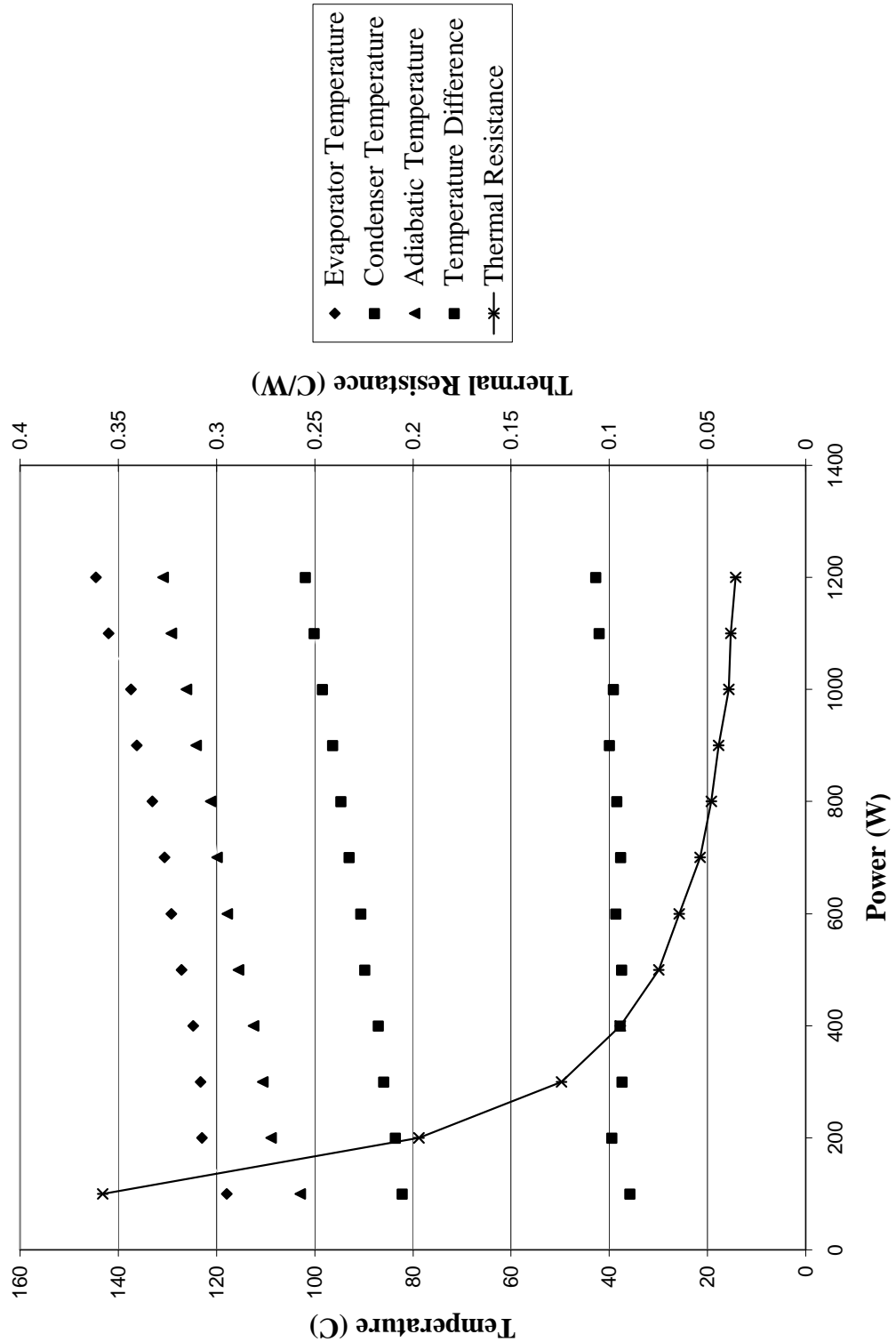


Fig 4.19 Power input effect on the heat transfer performance in the OHP and the thermal resistance of the OHP (cooling bath temperature = 80 °C, a filling ratio =70%, and tilted angle = 0 degrees)

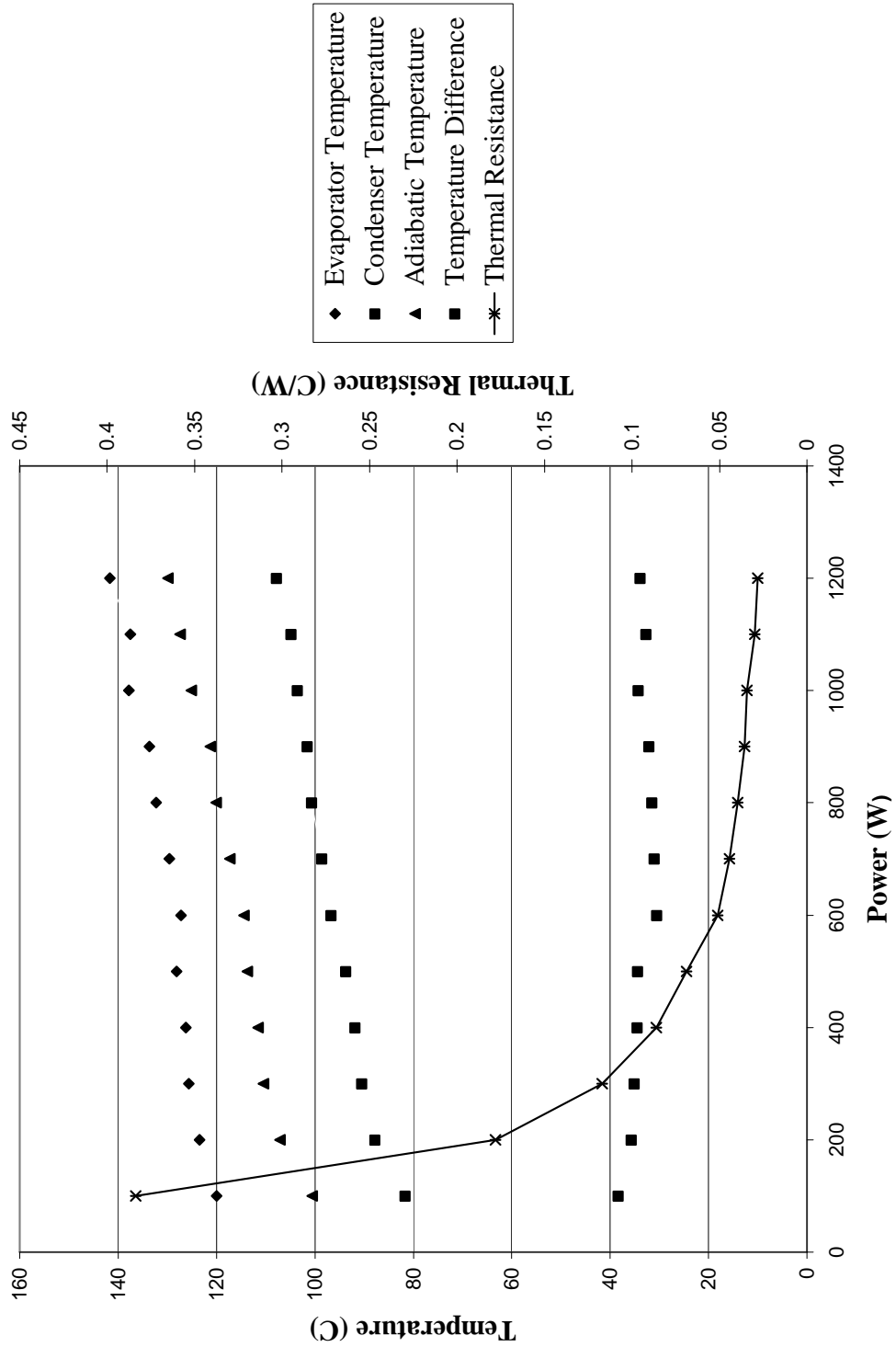


Fig 4.20 Power input effect on the heat transfer performance in the OHP and the thermal resistance of the OHP (cooling bath temperature = 80 °C, a filling ratio =70%, and tilted angle = -90 degrees)

As can be seen in figure 4.21 with the 70% filling ratio in the -90 position the system overall maintains a fairly even temperature distribution across the evaporator section when compared with the 50% filling ratio. The temperature spread that does occur is due to the oscillations of the fluid in the system. Some sections of the OHP have larger oscillations in temperature due to the distribution and size of the liquid plugs. The system maintains a temperature difference of 33 °C. It can also be seen that the evaporator and condenser temperatures are moving counter to each other during oscillations.

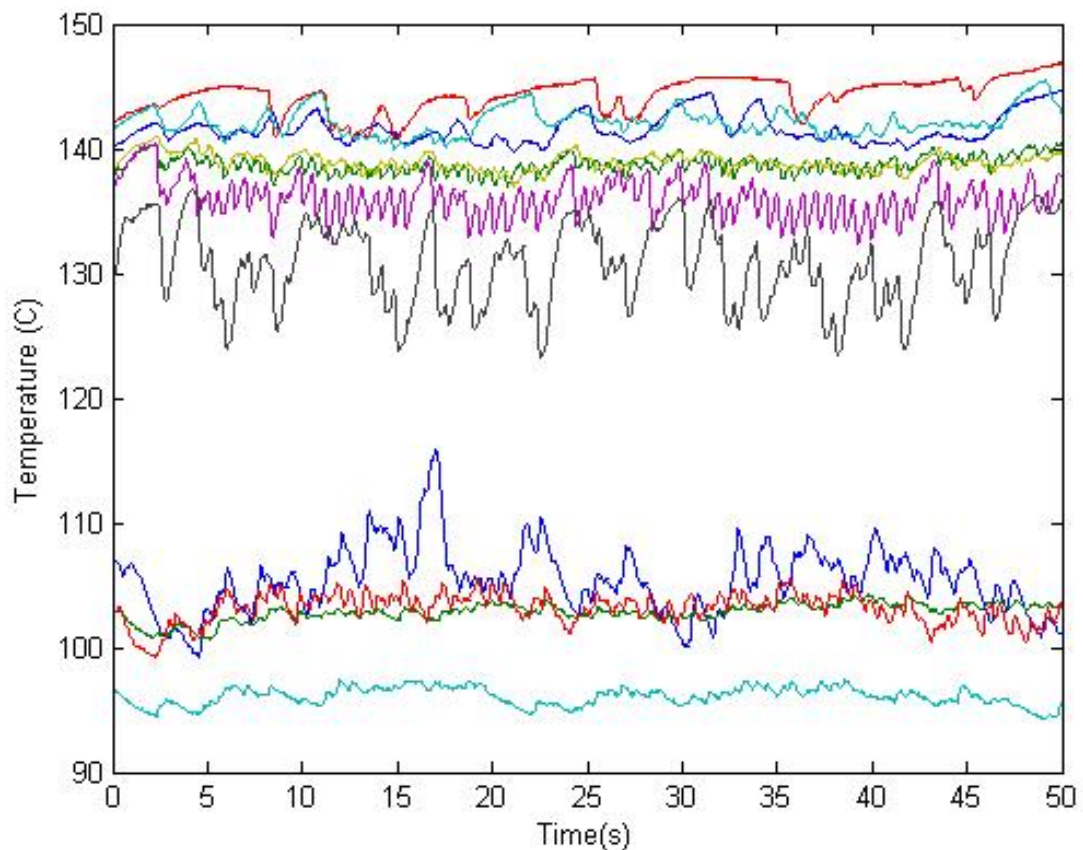


Fig 4.21 Temperature oscillations with respect to time; power input of 1200 watts, cooling bath temperature of 80C, position of -90 degrees, filling ratio of 70%

The 50% fill ratio however showed that the system had difficulty in maintaining an even temperature distribution in the evaporator section as can be seen in figure 4.22. This could be due to an uneven distribution of vapor bubbles. However after repeated usage of the system the vapor bubbles should have been more evenly distributed. The temperature difference is 42 °C which is much lower than at the other two cooling bath temperatures; however this is still 9 °C higher than the temperature difference for the 70% filling ratio. The large temperature spread in the %50 filling ratio is due to the lack of fluid available for adequate cooling to occur. This implies that the system is close to reaching dry out and no longer being able to oscillate.

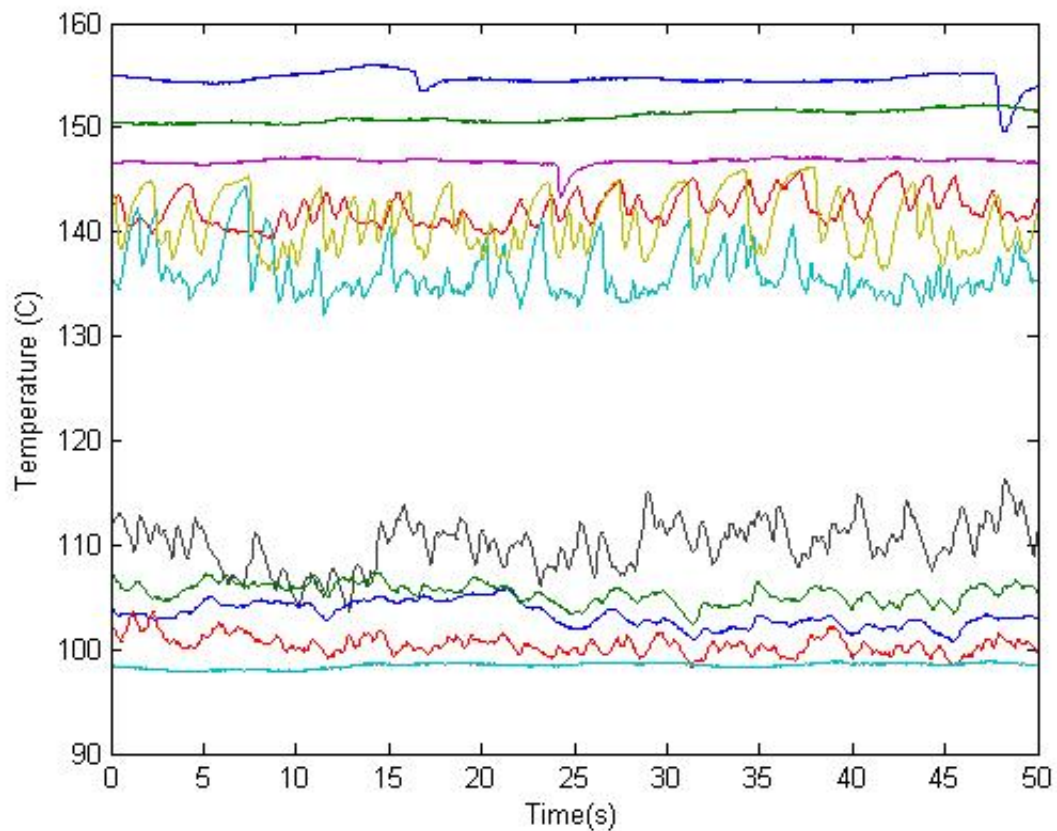


Fig 4.22 Temperature oscillations with respect to time; power input of 1200 watts, cooling bath temperature of 80C, position of -90 degrees, filling ratio of 50%

At the 0 degree position the system has a fairly large temperature difference of 42.7 °C which is very close to the temperature difference from the 50% filling ratio in the -90 position. From figure 4.23 it can be seen there is very even heating across the evaporator section and the size of the temperature oscillations are much smaller.

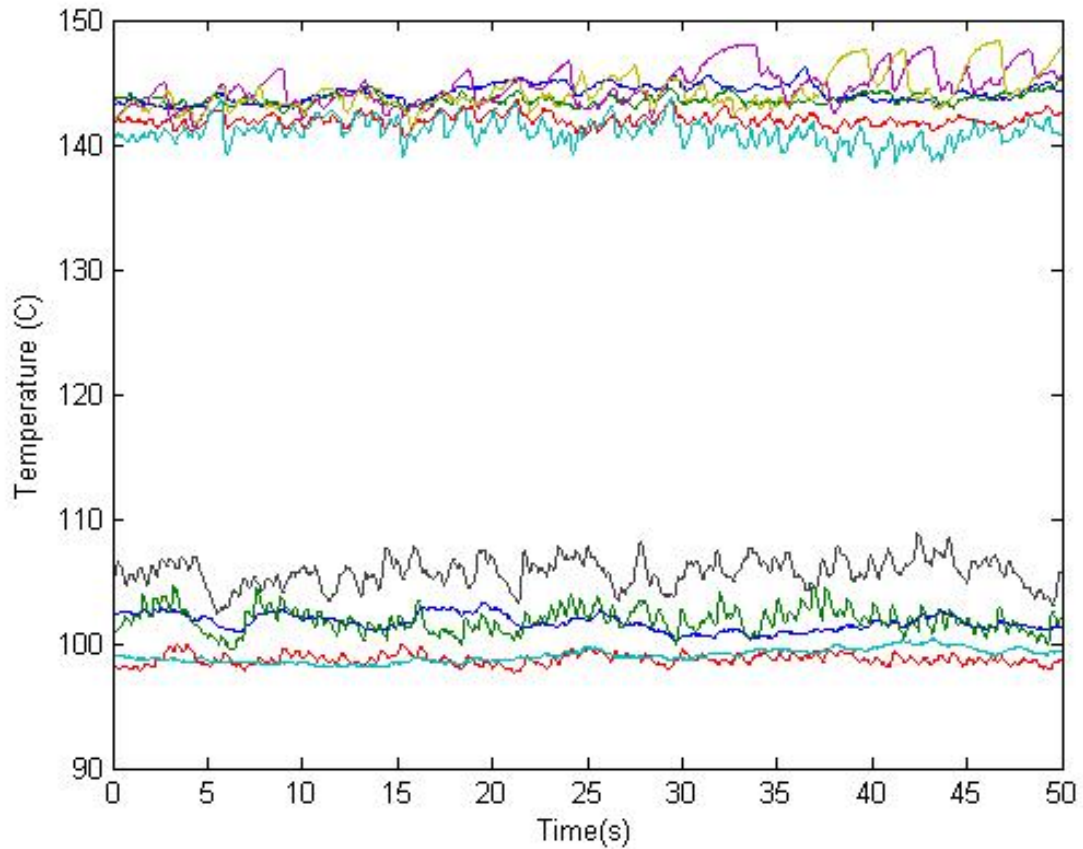


Fig 4.23 Temperature oscillations with respect to time; power input of 1200 watts, cooling bath temperature of 80C, position of 0 degrees, filling ratio of 70%

In the 90 degree position the oscillations also seems to be damped as can be seen in figure 4.24. The temperature difference decreases slightly to 39.9°C from the high seen in the 0 degree position.

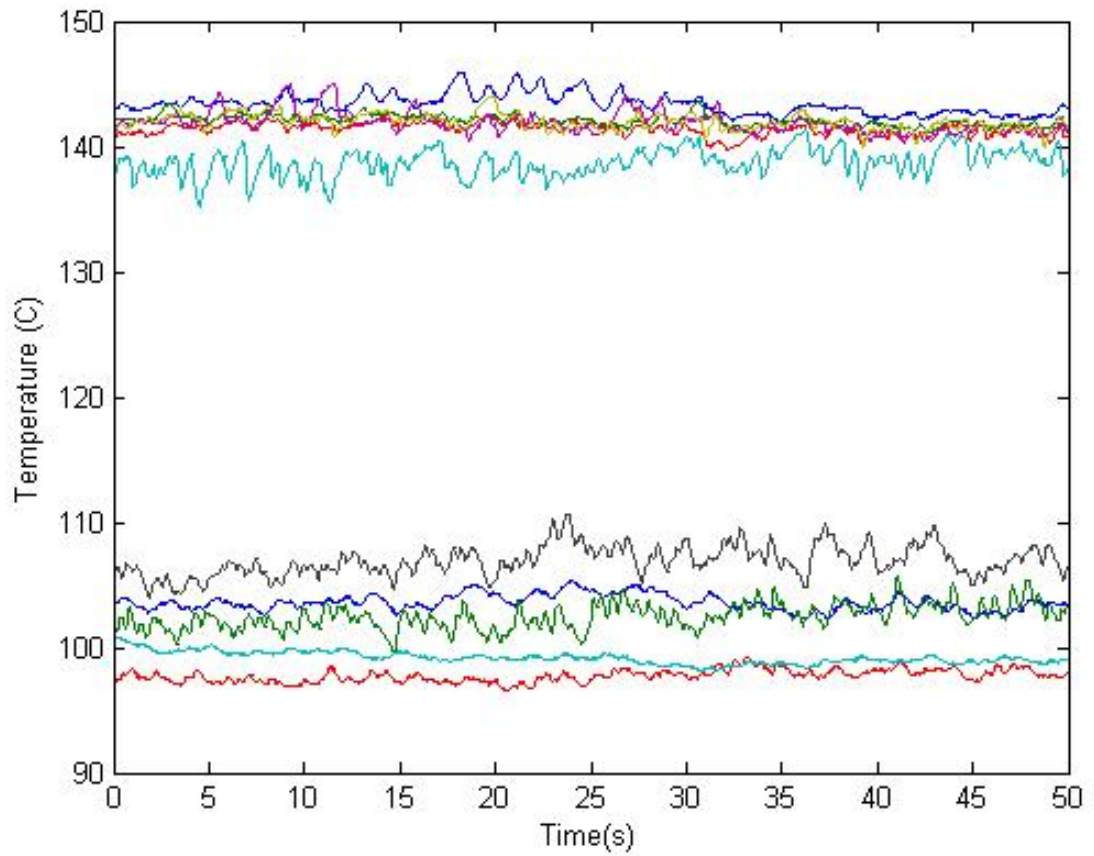


Fig 4.24 Temperature oscillations with respect to time; power input of 1200 watts, cooling bath temperature of 80C, position of 90 degrees, filling ratio of 70%

Chapter 5

Conclusions

An experimental investigation on oscillating heat pipes with uneven turns was conducted in order to determine the effect of short turns on the heat transport capability. The shorter turns do not go through both the evaporating and condensing sections. In one design, the short turns were placed on the evaporating section, i.e., 6-turns on the evaporating section and 3 turn on the condensing section. Experimental results show that even when the evaporation section was on the bottom and cooling section on the top the OHP had a thermal resistance of $1.44^{\circ}\text{C}/\text{W}$ at a heat input of 50 watts with a condensing temperature of 20°C . As can be seen while the heat pipe can function, the heat pipe cannot reach a high effective thermal conductivity. The primary reason for this is that the effective increase in size of the evaporator will not help to increase the heat transport capability in an OHP because the thermal resistance in the condenser was significantly increased.

The second design of the OHP with short turns consists of 14 long turns and 6 short turns. The 14 long turns run from the evaporator to the condenser and 6 short turns were placed only on the evaporating section. An extensive experimental investigation on the effects of the input power, tilted angle, condensing temperature, and charging ratio was conducted. Experimental results show that for all test conditions, the OHP functions very well and it can transport an input power up to 1200 W and can reach a thermal resistance of $0.028^{\circ}\text{C}/\text{W}$. From the experimental results of tilted angle effect, it can be

found that the heat pipe is almost independent of the tilted angle. Most importantly, it is shown that with a number of short turns placed on the evaporating section, the OHP can operate efficiently without the assistance of the gravitational force. In other words, the heat pipe developed herein can operate at a condition of the heating section on the top and the cooling section on the bottom with a distance of 18.5 cm from the center of the evaporator section the center of the condensing section. In addition, the results show that the heat transfer performance depends on the operating temperature and charging ratio. When the operating temperature increases, the heat transfer performance of the OHP investigated herein significantly increase. The heat transfer performance in an OHP with a filling ratio 70% is much better than that with 50%.

References

1. Akachi, H., 1990, "Structure of a Heat Pipe," U.S. Patent 4,921,041
2. Khandekar, S., Cui, X., and Groll, M., 2002, "Thermal Performance Modeling of Pulsating Heat Pipes by Artificial Neural Network," Heat Pipe Science Technology Application, Proceedings of the 12th International Heat Pipe Conference, Moscow, Russia, May 19-24, Russian Academy of Sciences, pp. 215-219
3. Shafi, M., Fahri, A., and Zhang, Y., 2001 "Thermal Modeling of Unlooped and Looped Pulsating Heat pipes," ASME Journal of Heat Transfer, Vol. 123, pp. 1159-1172.
4. Khandekar, S., Schneider, M., Schafer, P. Kulenovic, R., and Groll, M., 2002, "Thermofluid dynamic study of flat-plate closed-loop pulsating heat pipes," *Microscale Thermophysical Engineering*, **6**, 303-317.
5. Charoensawan, P., Khandekar, S., Groll, M., and Terdtoon, P., Closed Loop Pulsating Heat Pipes, Part A: Parametric Experimental Investigations, Applied Thermal Engineering, vol. 23, no. 16, pp. 2009–2020, 2003.
6. Zhang X. M., Xu, J. L., and Zhou, Z. Q., Experimental Study of a Pulsating Heat Pipe using FC-72, Ethanol, and Water as Working Fluids, Experimental Heat Transfer, vol. 17, no. 1, pp. 47–67, 2004.
7. Ma, H. B., Hanlon, M. A., and Chen, C. L., An Investigation of Oscillating Motions in a Miniature Pulsating Heat Pipe, Journal of Microfluidics and Nanofluidics, vol. 2, pp. 171–179, 2006.
8. Miyazaki, Y., and Akachi, H., Heat Transfer Characteristics of Looped Capillary Heat Pipe, Proc. 5th International Heat Pipe Symposium, pp. 378–383, Melbourne, Australia, 1996.
9. Zhang, Yuwen and Faghri, Amir (2008) "Advances and Unsolved Issues in Pulsating Heat Pipes", Heat Transfer Engineering, 29:1, 20 — 44
10. Wilson, C., Borgmeyer, B., Winholtz, R. A., Ma, H. B., Jacobsen, D., Hussey, D., "Thermal and Visual Observation of Eater and Acetone Oscillating Heat Pipes".
11. Thompson, S., Wilson, C., B., Winholtz, R. A., Ma, H. B., Jacobsen, D., Hussey, D., "Experimental Investigation of Miniature Three-Dimensional Flat-Plate Oscillating Heat Pipe", Journal of Heat Transfer, vol. 131, 2009.